Evaluations of nuclear weak rates relevant to astrophysical applications

Toshio Suzuki
Nihon University, Tokyo

ICNT 2015, MSU

May 25, 2015

○ New shell-model Hamiltonians

SFO (p-shell), GXPF1J (fp-shell), USDB (sd-shell)

Spin modes -GT strengths, M1 moments- are well described.

→ Accurate evaluation of spin-dependent transition rates

○ ν-nucleus reactions

- ν-^{12}C, ν-^{56}Fe, ν-^{56}Ni reactions with SFO and GXPF1J
- Nucleosynthesis of light elements, ^{7}Li and ^{11}B, and ^{55}Mn in supernova explosions (SNe)

  ν oscillations effects and ν oscillation parameters
- ν-^{40}Ar reactions with VMU (monopole-based universal interaction)

○ e-capture and β-decay rates in stellar environments

- e-capture rates in pf-shell nuclei with GXPF1J

  Type-Ia supernova explosions and nucleosynthesis
- e-capture and β-decay rates in sd-shell and pf-shell nuclei and cooling of stars by URCA processes
- β-decay half-lives of waiting-point nuclei at N=126 and r-process nucleosynthesis

○New shell-model Hamiltonians and successful description of Gamow-Teller (GT) strengths

SFO (p-shell): GT in ^{12}C, ^{14}C

Suzuki, Fujimoto, Otsuka, PR C69, (2003)

GXPF1J (fp-shell): GT in Fe and Ni isotopes, M1 strengths

Honma, Otsuka, Mizusaki, Brown, PR C65 (2002); C69 (2004)
Suzuki, Honma et al., PR C79, (2009)

VMU (monopole-based universal interaction)

Otsuka, Suzuki, Honma, Utsuno et al., PRL 104 (2010) 012501

* important roles of tensor force

Monopole terms of V_{NN}

$$V_M^T(j_1 j_2) = \frac{\sum_J (2J+1) < j_1 j_2; JT | V | j_1 j_2; JT >}{\sum_J (2J+1)}$$

$j_> - j_<$: attractive

$j_> - j_>, j_< - j_<$: repulsive

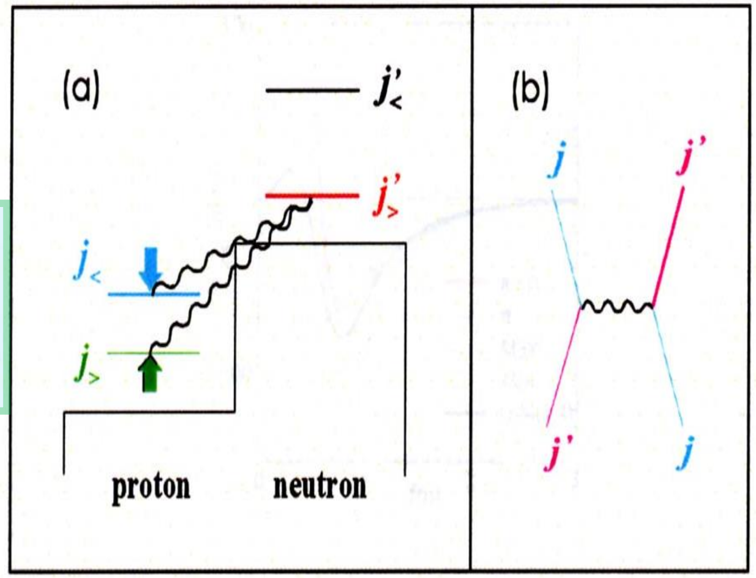

Otsuka, Suzuki, Fujimoto, Grawe, Akaishi, PRL 69 (2005)

Monopole terms: New SM interactions vs. microscopic G matrix

tensor force

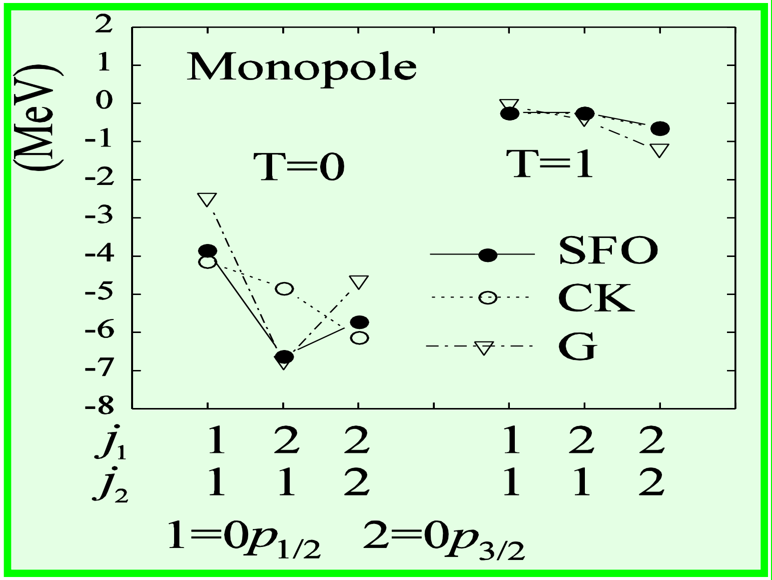

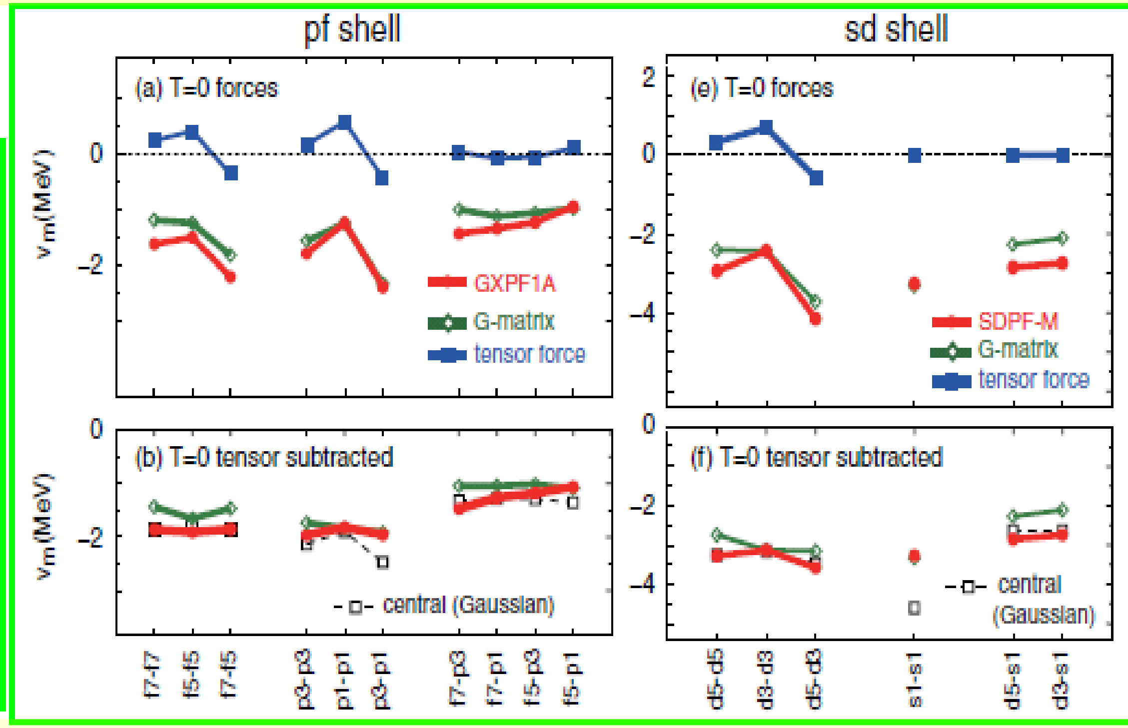

Proper shell evolutions toward drip-lines: Change of magic numbers

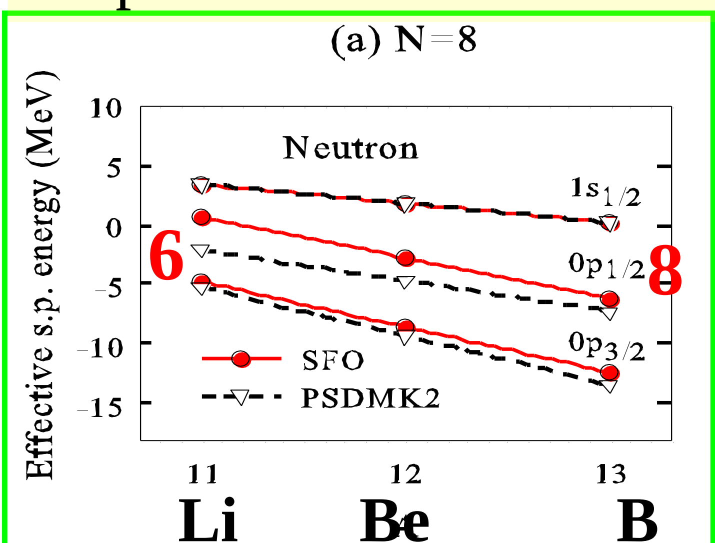

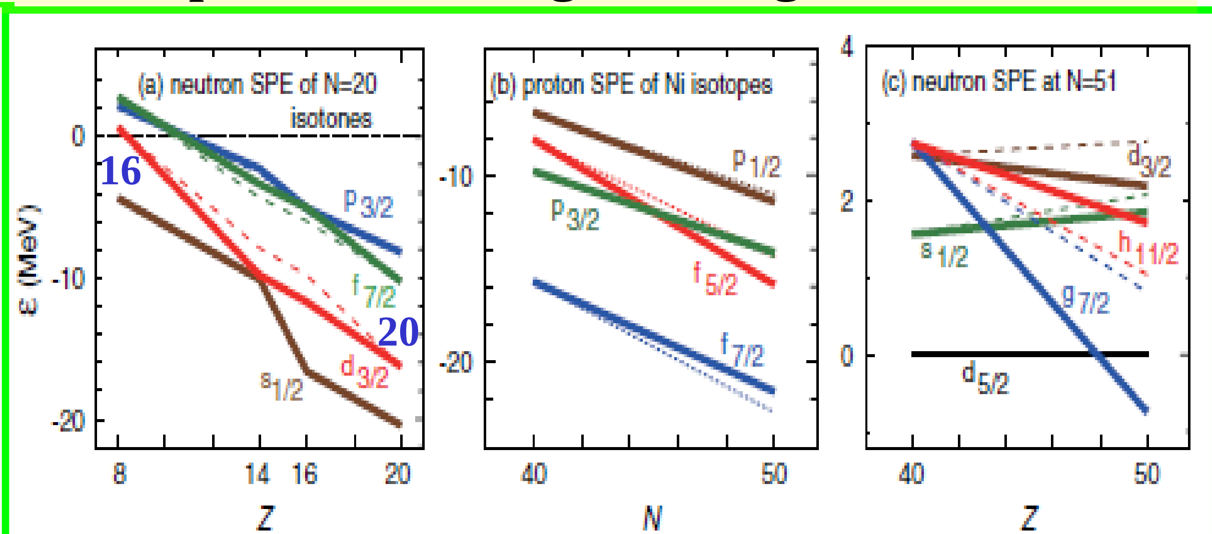

B(GT) values for ^{12}C -> ^{12}N

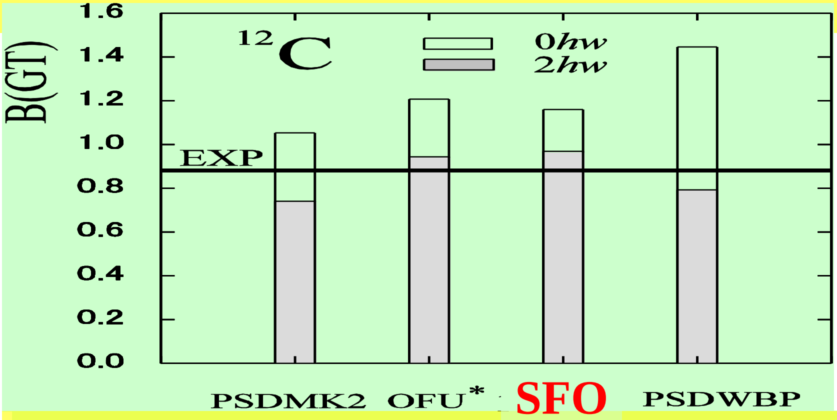

B(GT) values for ^{14}N -> ^{14}C

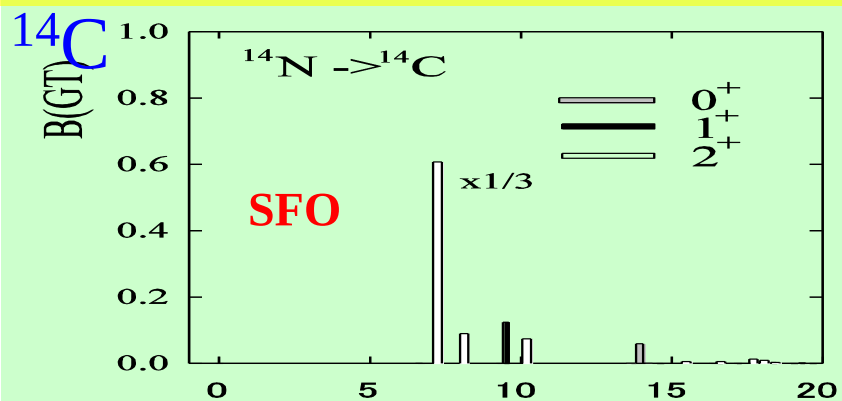

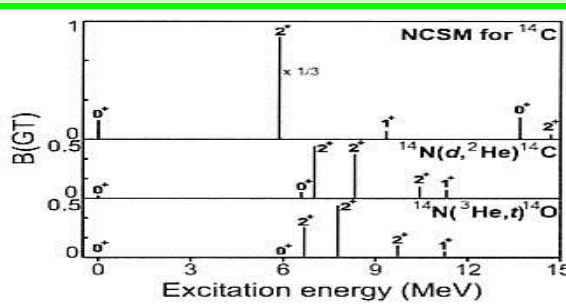

FIG. 3. Experimental B(GT) distributions, compared to the theoretical result of Aroua *et al.* [14], where the B(GT) to the 2^+ state was scaled down by a factor of 3.

Negret et al., PRL 97 (2006)
KVI
RCNP

Magnetic moments of p-shell nuclei

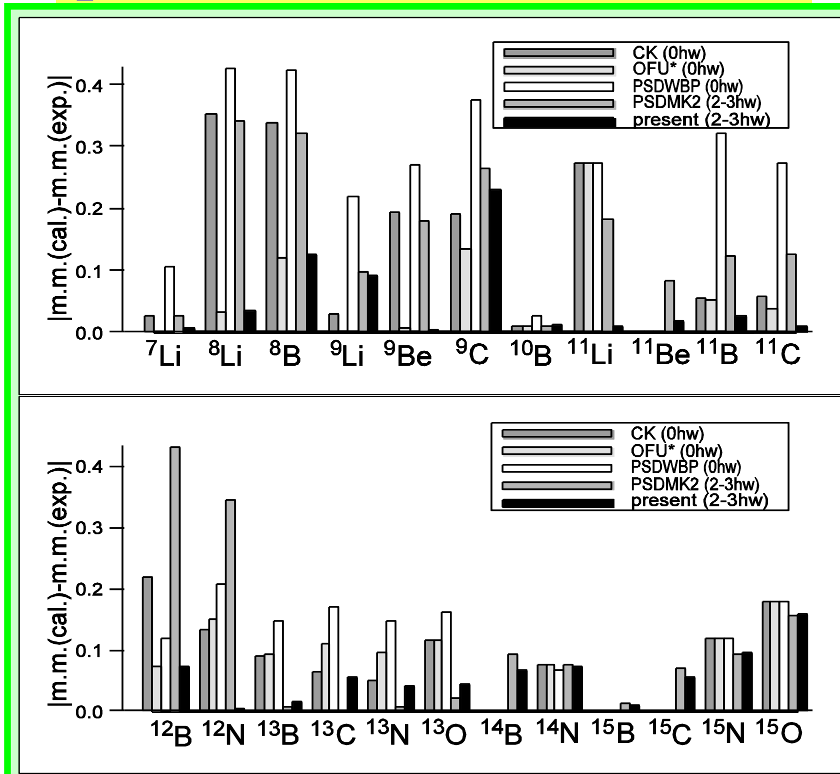

present = SFO Suzuki, Fujimoto, Otsuka, PR C67 (2003)

Space: up to 2-3 hw

SFO*: g_A^{eff}/g_A=0.95

B(GT: ^{12}C)_cal = experiment

New shell-model Hamiltonians in fp-shell and spin responses

GXPF1: Honma et al., PR C65 (2002); C69 (2004); A = 47-66

KB3: Caurier et al., Rev. Mod. Phys. 77, 427 (2005)

KB3G A = 47-52 KB + monopole corrections

- **Spin properties of fp-shell nuclei are well described**

M1 strength (GXPF1J)

$B(GT_-)$ for ^{58}Ni

$g_A^{eff}/g_A^{free}=0.74$

$g_S^{eff}/g_S=0.75\pm0.2$

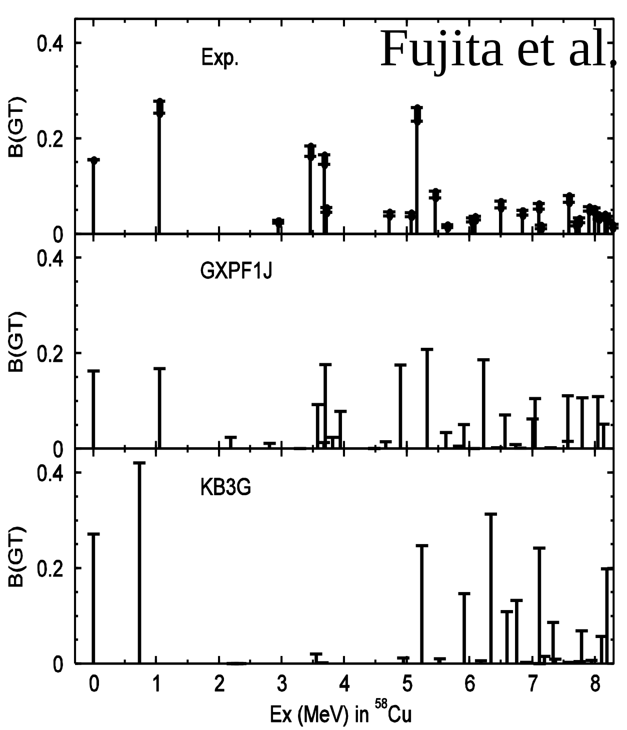

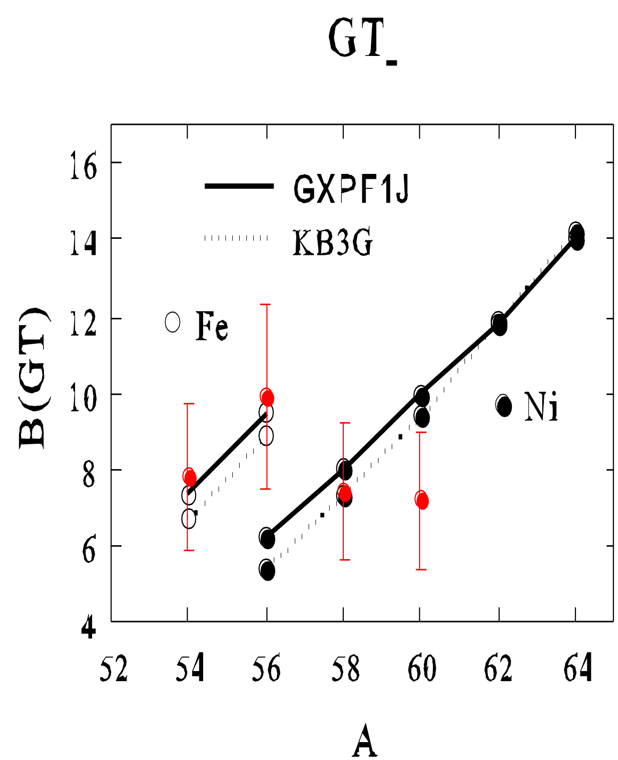

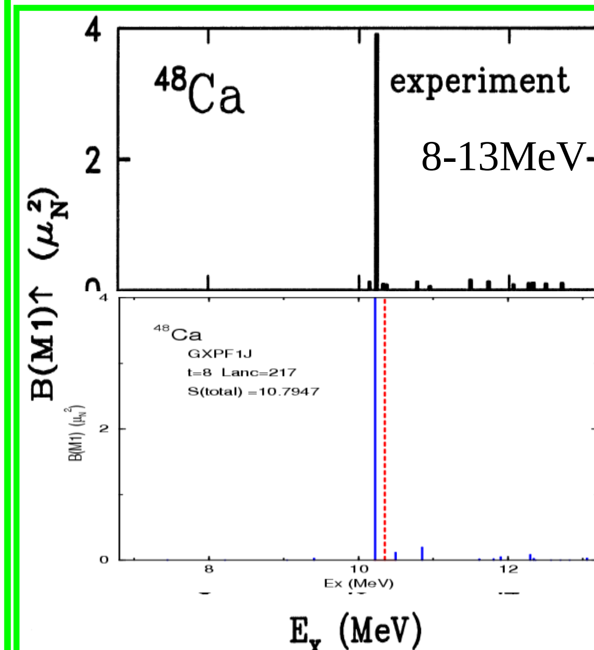

○ ν-nucleus reactions

p-shell: SFO

pf-shell: GXPF1J (Honma et al.)

cf. KB3 Caurier et al.

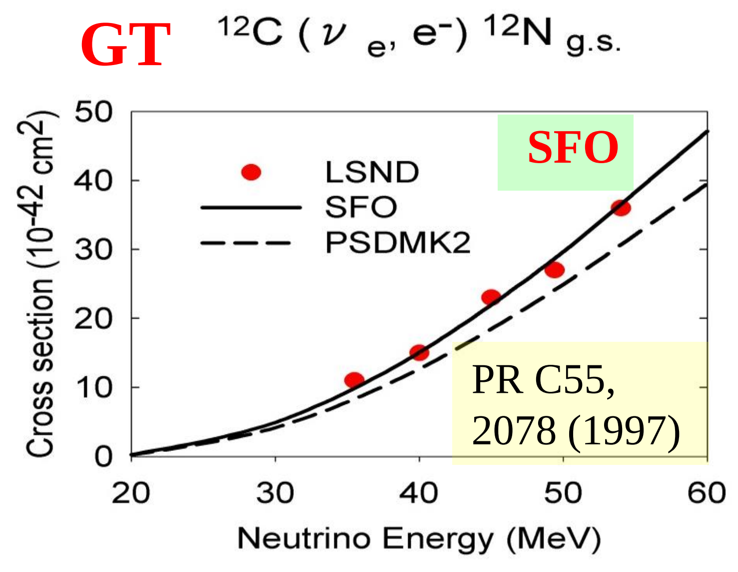

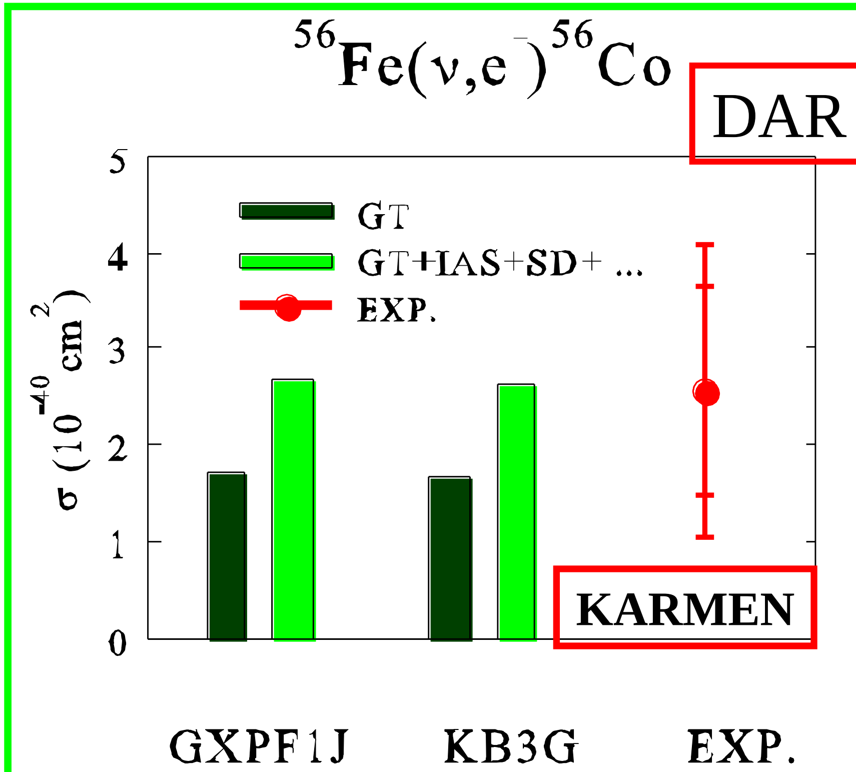

Suzuki, Chiba, Yoshida, Kajino, Otsuka, PR C74, 034307, (2006).

SFO: g_A^{eff}/g_A=0.95
B(GT: 12C)_cal = experiment

(ν, ν'), (ν_e, e^-) SD exc.
SFO reproduces DAR cross sections

B(GT)=9.5 B(GT)$_{exp}$=9.9±2.4 B(GT)$_{KB3G}$=9.0

SD + … : RPA (SGII)

$$\langle\sigma\rangle_{exp} = (256 \pm 108 \pm 43) \times 10^{-42}\ \mathrm{cm}^2.$$
$$\langle\sigma\rangle_{th} = (258 \pm 57) \times 10^{-42}\ \mathrm{cm}^2.$$

SM(GXPF1J)+RPA(SGII)	259 x10 $^{-42}$cm^2
RHB+RQRPA(DD-ME2)	263
RPA(Landau-Migdal force)	240

Nucleosynthesis processes of light elements

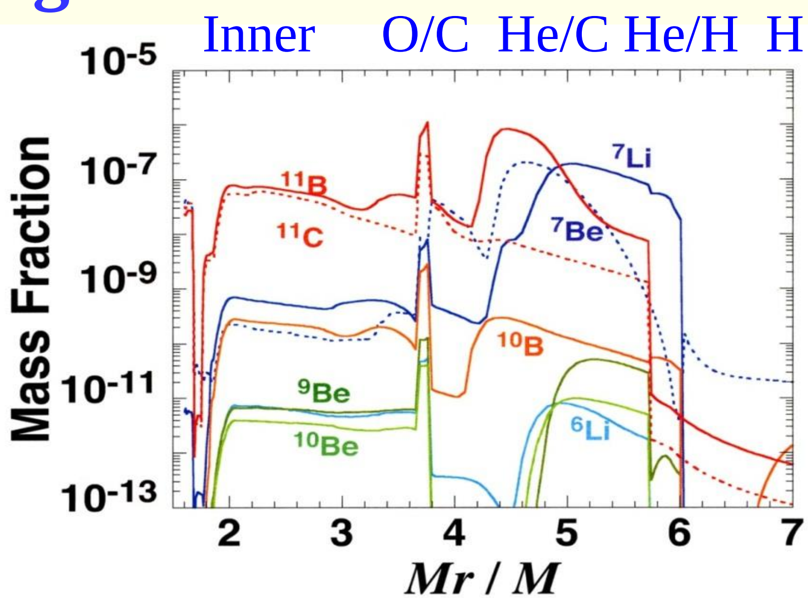

Fig. 4.— Mass fraction distribution of Model 1. The mass fractions of ^{7}Li and ^{7}Be, and ^{11}B and ^{11}C are separated.

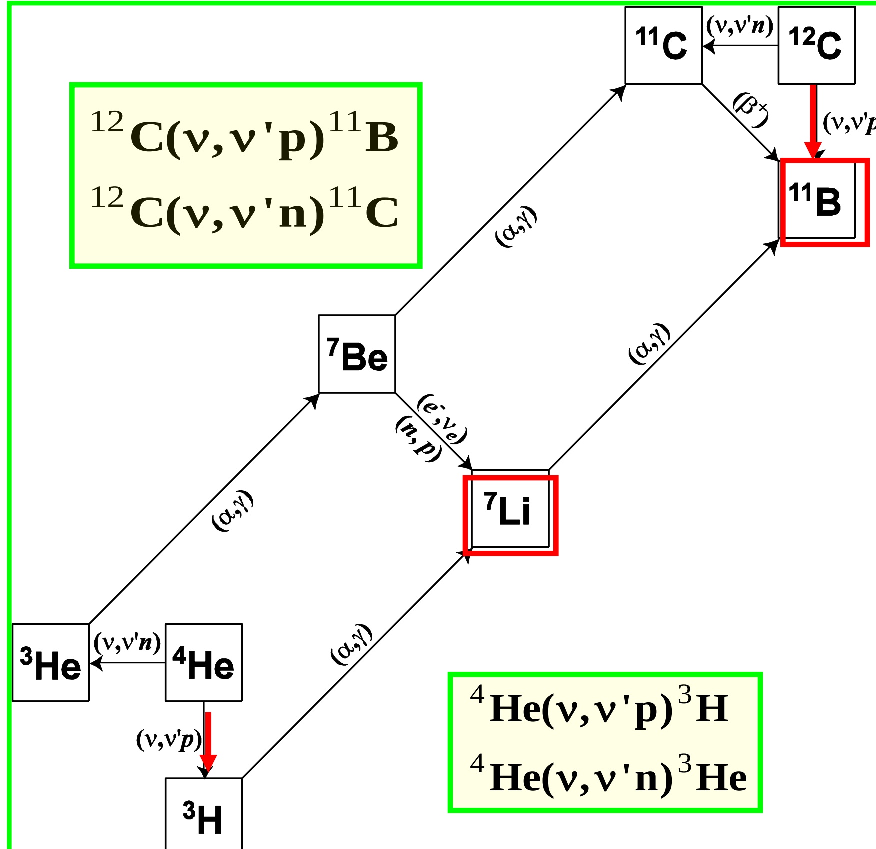

$^{12}C(\nu,\nu'p)^{11}B$

$^{12}C(\nu,\nu'n)^{11}C$

$^{4}He(\nu,\nu'p)^{3}H$

$^{4}He(\nu,\nu'n)^{3}He$

Enhancement of ^{11}B and ^{7}Li abundances in supernova explosions

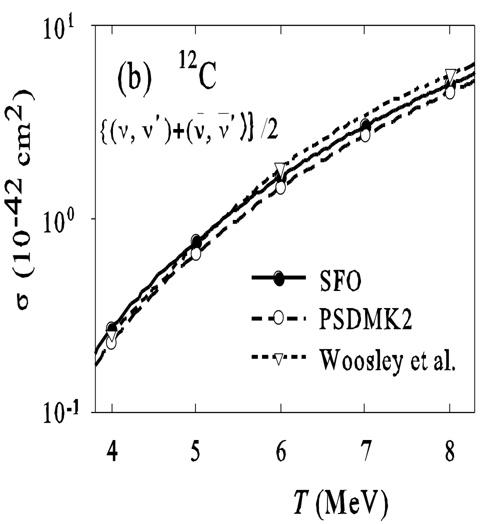

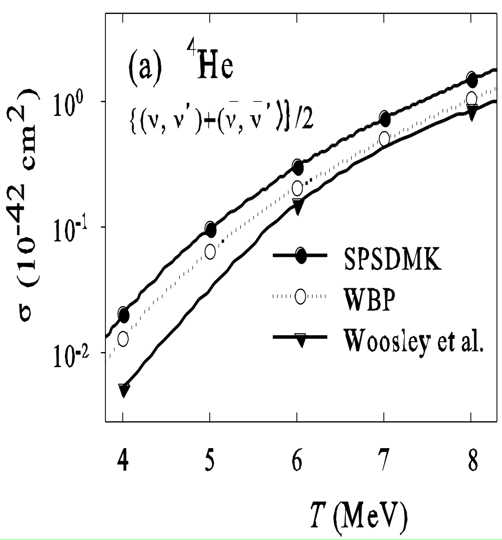

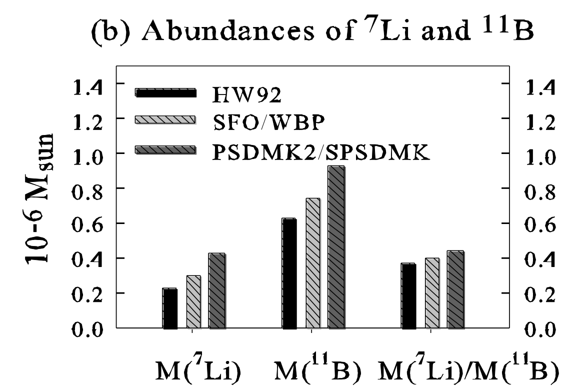

MSW ν oscillations

Normal hierarchy | Inverted hierarchy

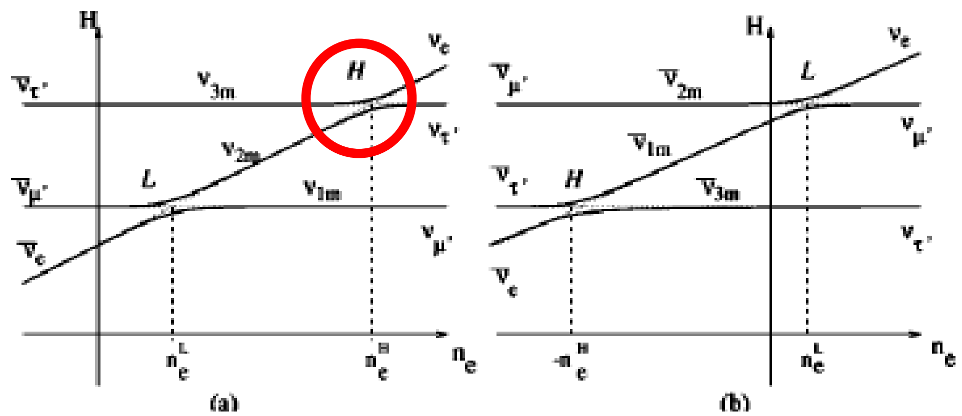

$$\text{Normal-hierarchy}: \nu_\mu, \nu_\tau \rightarrow \nu_e$$

Increase in the rates
4He(ν_e,e^-p)3He
12C(ν_e,e^-p)11C
in the He layer

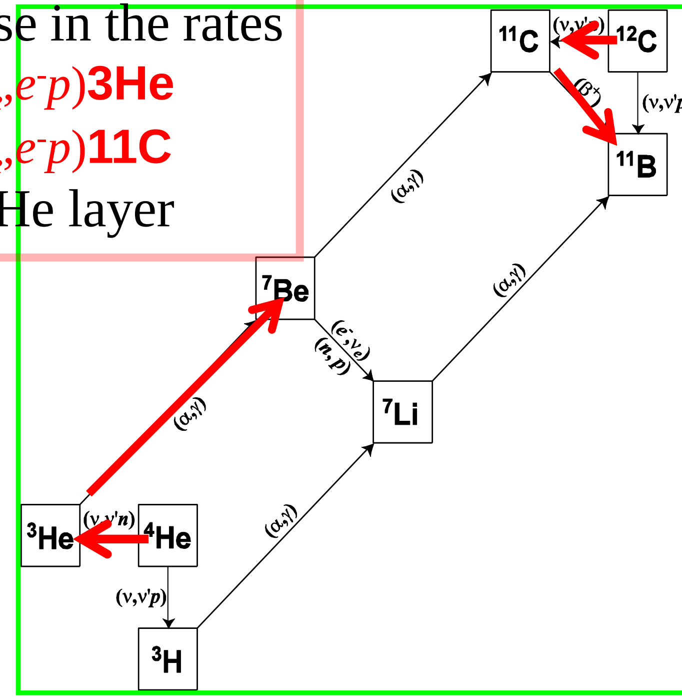

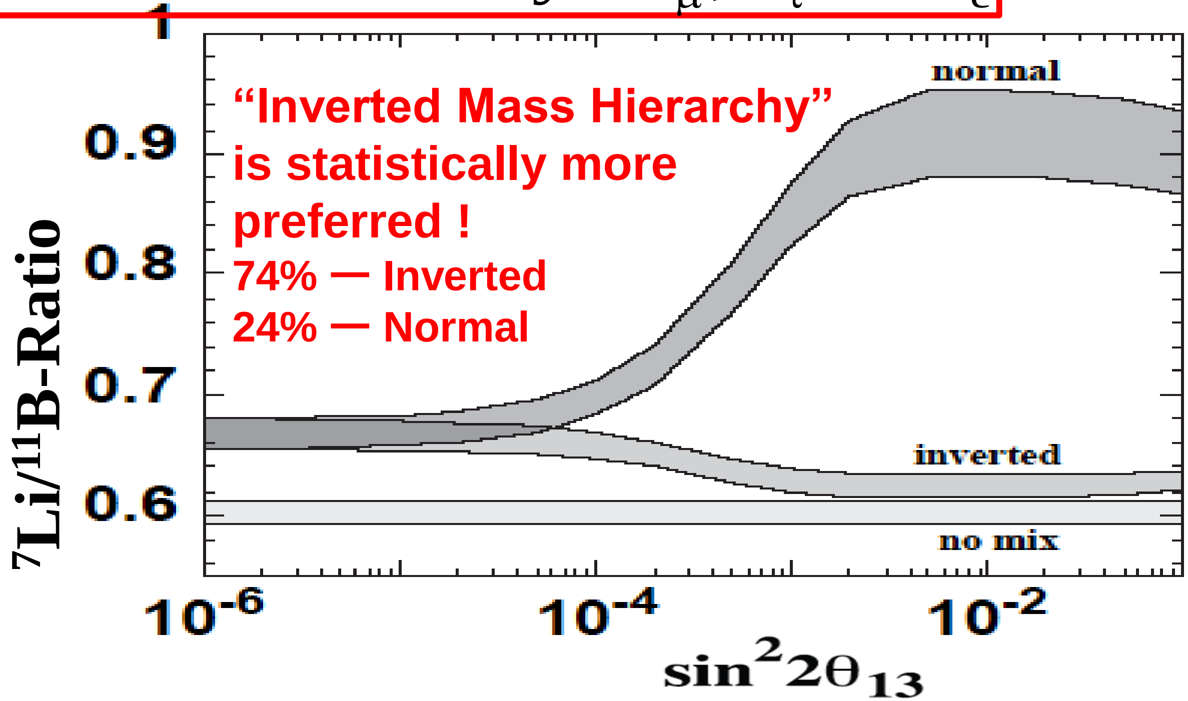

"Inverted Mass Hierarchy" is statistically more preferred !
74% — Inverted
24% — Normal

- T2K, MINOS (2011)
- Double CHOOZ, Daya Bay, RENO (2012)

$\sin^2 2\theta_{13} = 0.1$

First Detection of ^{7}Li/^{11}B in SN-grains in Murchison Meteorite
W. Fujiya, P. Hoppe, & U. Ott, ApJ 730, L7 (2011).

Bayesian analysis:
Mathews, Kajino, Aoki and Fujiya, Phys. Rev. D85,105023 (2012).

- Effects of MSW ν-oscillations
  normal hierarchy: high res. + low res. → $^7Li/^{11}B$ enhanced
  inverted-hierarchy: no high-res. → $^7Li/^{11}B$ not enhanced
  Supernova X-grains in Murchison meteorite
  → inverted hierarchy is statistically favored
  W. Fujiya, P. Hoppe, & U. Ott, ApJ 730, L7 (2011).
  Mathews, Kajino, Aoki and Fujiya, Phys. Rev. D85,105023 (2012).

- New ν-^{13}C cross sections with SFO
  ^{13}C is a good target for low-energy ν detection; E<10 MeV
  Suzuki, Balantekin and Kajino, PR C86, 015502 (2012)

- New ν-^{16}O cross sections with SFO-tls
  Full inclusion of tensor force in p-sd cross shells:
  tensor → $\pi+\rho$ LS → $\sigma+\rho+\omega$
  Spin-dipole transitions (0^-, 1^-, 2^-)
  Excitation energies of the spin-dipole states are improved.

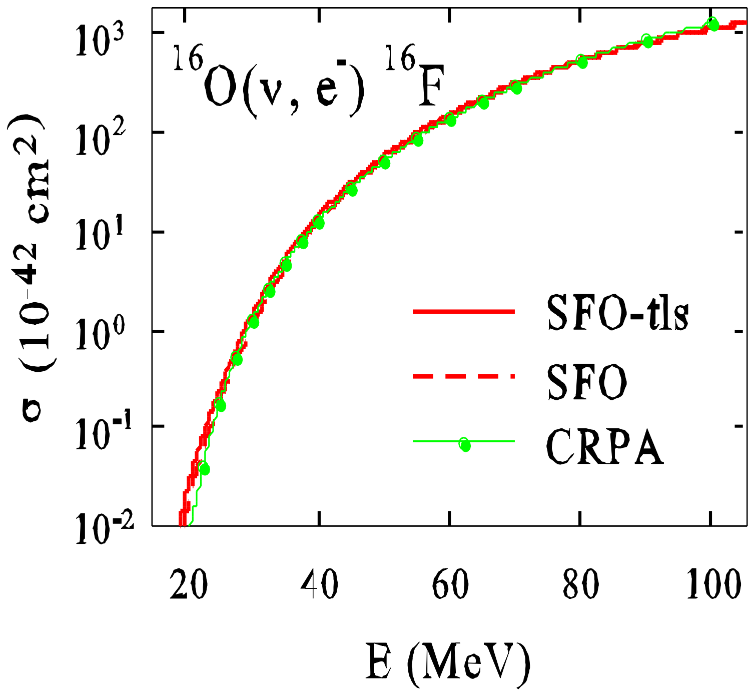

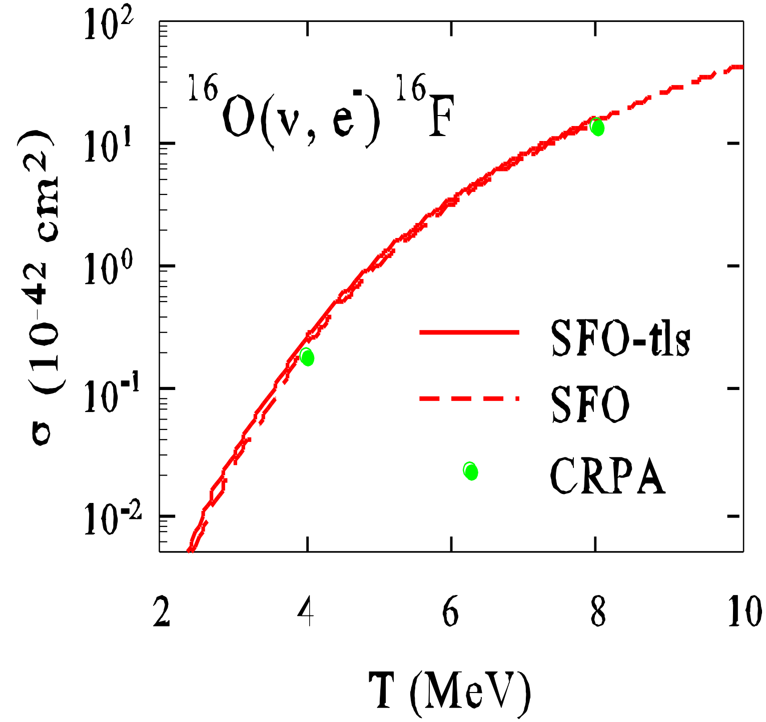

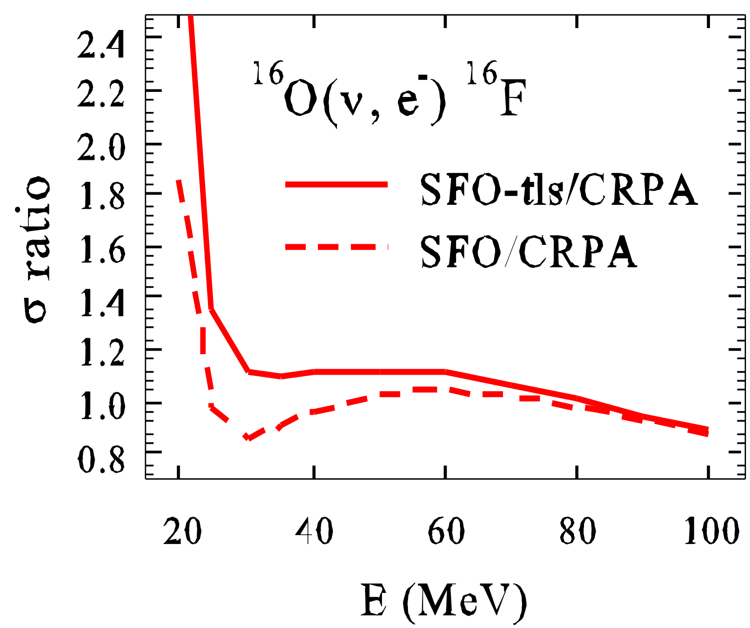

T= temperature of supernova ν

T	σ(SFO-tls)/σ(CRPA):
4	1.41
8	1.17

g_A^{eff}/g_A=0.95

CRPA: Kolbe, Langanke & Vogel, PR D66 (2002)

Soft dipole resonance in ^{11}Li

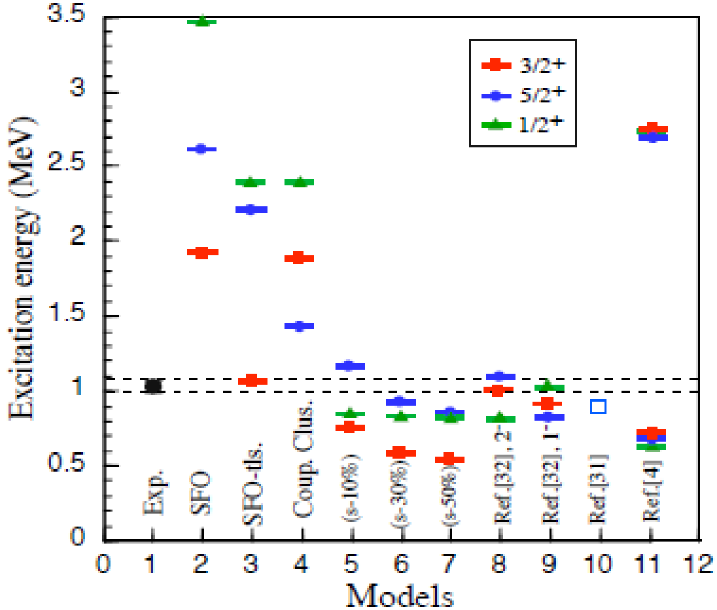

FIG. 4: The experimental excitation energy compared with different theoretical model predictions. 1=experimental data, Shell model with 2= SFO and 3=SFO-tls interactions, 4=Coupled Cluster, 5,6,7=three-body model with $2s_{1/2}$, 10%, 30% and 50%, respectively, 8=Ref.[32] with ^{10}Li(2^-), 9=Ref.[32] with ^{10}Li(1^-),10=Ref.[31] and 11=Ref.[4]. The red (squares), blue (circles), green (triangles) lines represent states with spin $3/2^+$, $5/2^+$, $1/2^+$, respectively.

^{11}Li (d, d') ^{11}Li

Kanungo et al., PRL, in press

Isoscalar E1 transition density

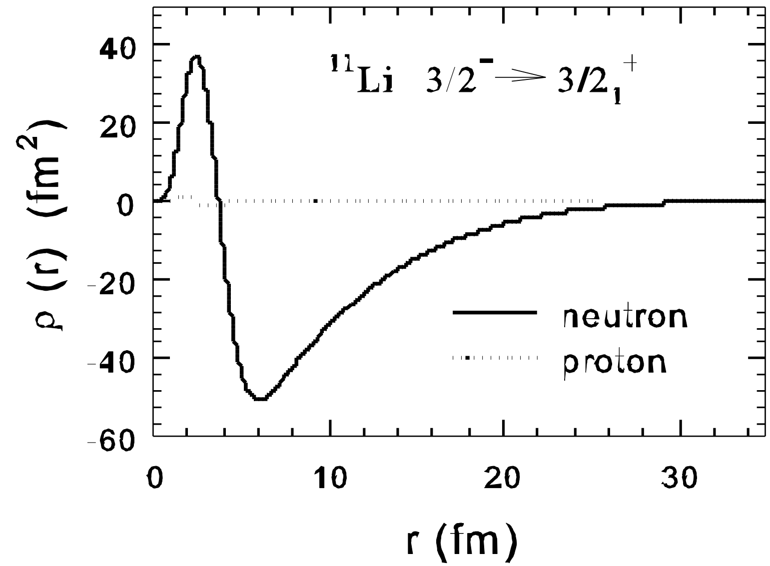

IV E1 transition density

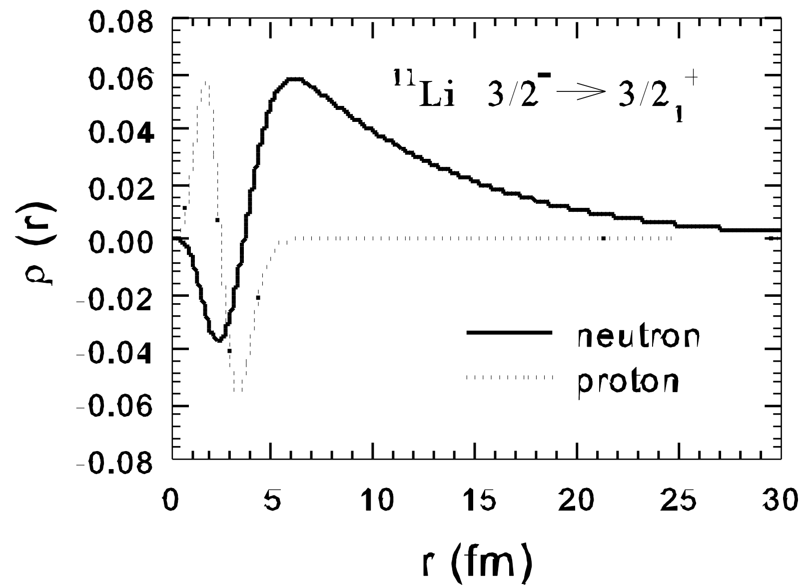

▪ ν- ^{40}Ar reactions

Liquid argon = powerful target for SNν detection

VMU= Monopole-based universal interaction

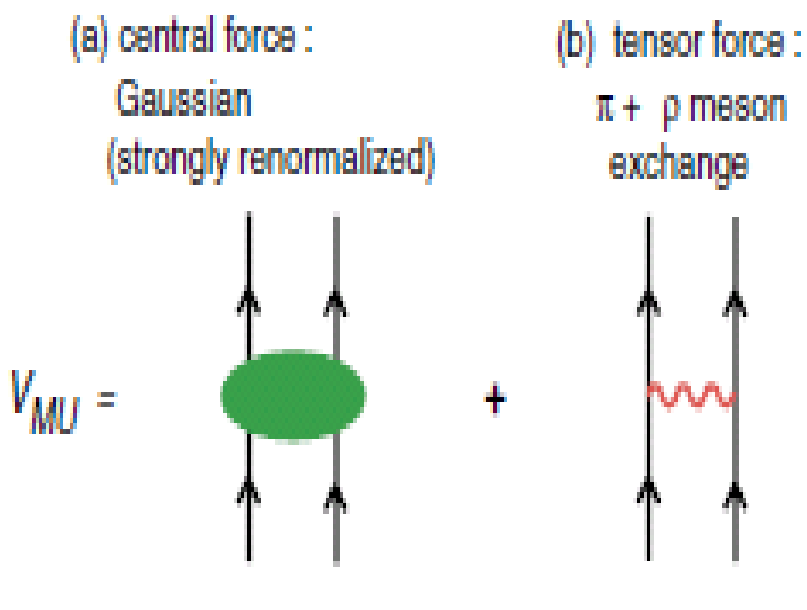

FIG. 2 (color online). Diagrams for the V_{MU} interaction.

Important roles of tensor force

Otsuka, Suzuki, Honma, Utsuno, Tsunoda, Tsukiyama, Hjorth-Jensen PRL 104 (2010) 012501

tensor force: bare≈renormalized

○ sd-pf shell: **^{40}Ar (ν, e$^-$) ^{40}K**

SDPF-VMU-LS

sd: SDPF-M (Utsuno et al.)

fp: GXPF1 (Honma et al.)

sd-pf: VMU + 2-body LS

$(sd)^{-2}$ $(fp)^2$: 2hw

B(GT) & ν-^{40}Ar cross sections

Solar ν cross sections folded over ^{8}B ν spectrum

Suzuki and Honma, PR C87, 014607 (2013)

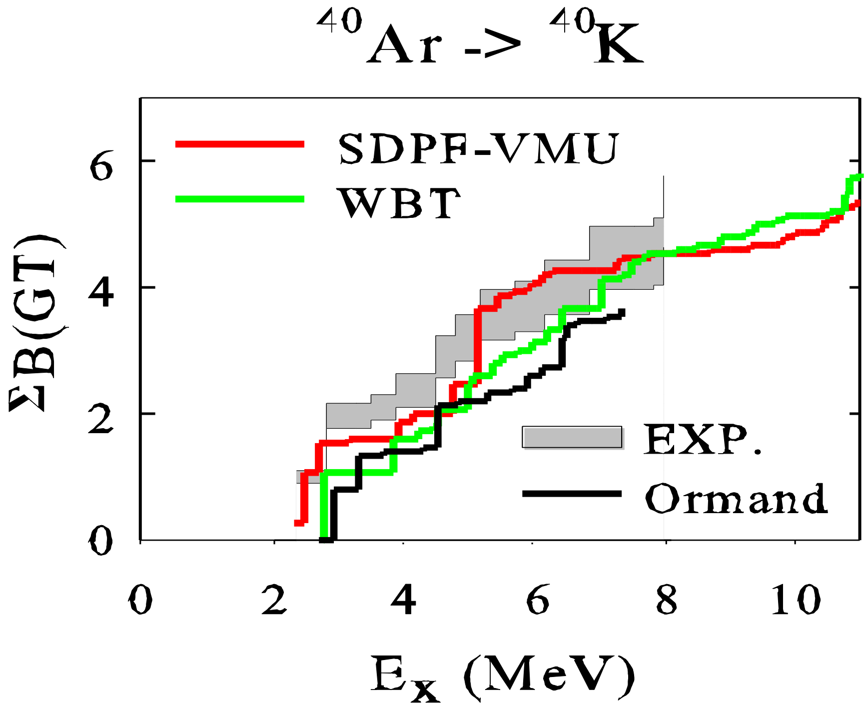

(p,n) Bhattacharya et al., PR C80 (2009)

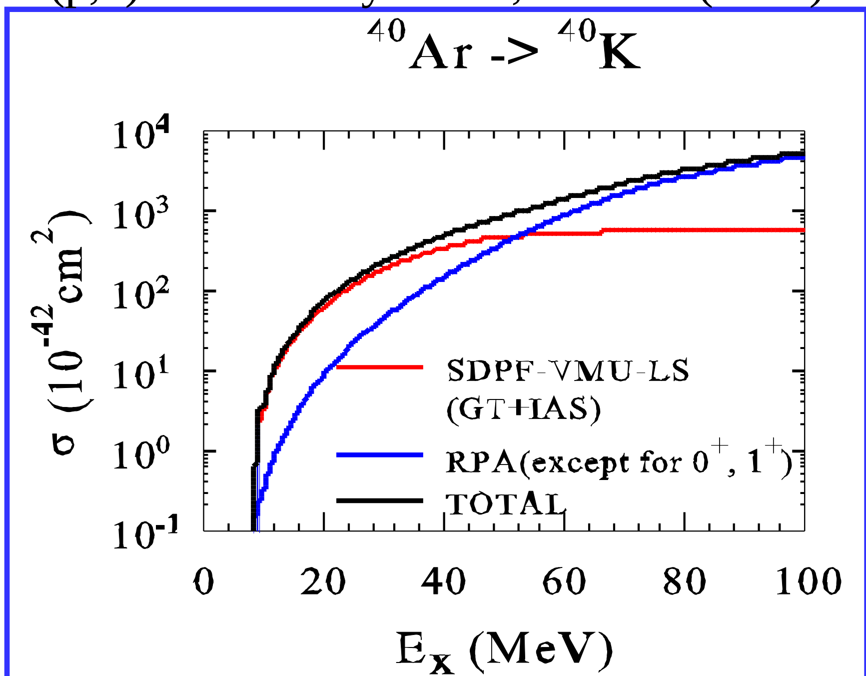

Solar ν cross sections folded over ^{8}B ν spectrum

^{40}Ar (ν, e^-) ^{40}K

GT+IAS

E_e > 5 MeV : ICARUS

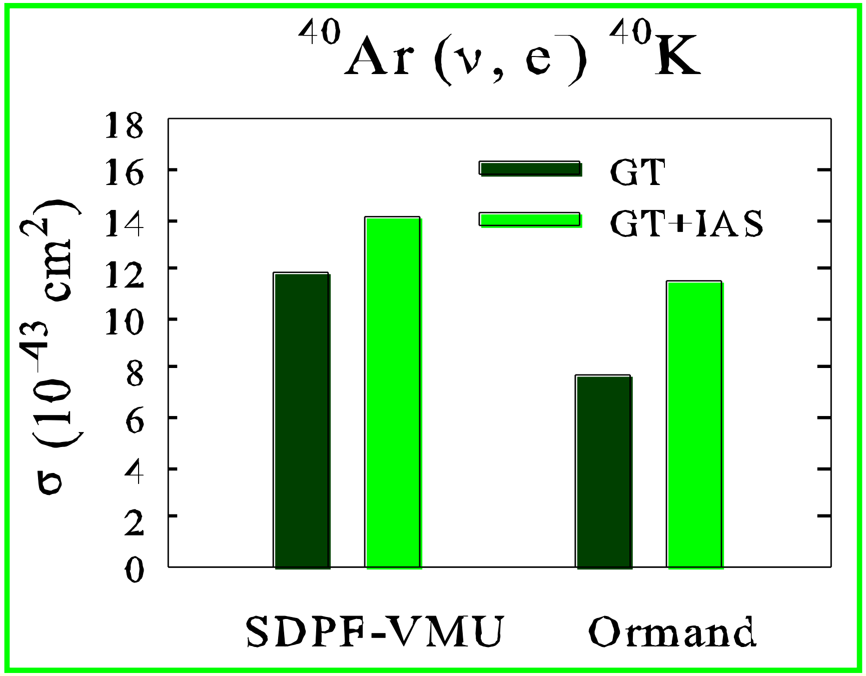

IAS: C0+L0 ≈$[(q^2-\omega^2)/q^2]^2 \times$ C0 ; $^+$ C0 only

GT: E_1^5 +M1+C_1^5+L_1^5 ; $^+$ E_1^5 only

$^+$Ormand et al, PL B345, 343 (1995)

PHYSICAL REVIEW C 89, 064313 (2014)

Gamow-Teller transitions in the $A = 40$ isoquintet of relevance for neutrino captures in ^{40}Ar

M. Karakoç,[1,2] R. G. T. Zegers,[3,4,5,*] B. A. Brown,[3,4,5] Y. Fujita,[6,7] T. Adachi,[6] I. Boztosun,[1,2] H. Fujita,[6] M. Csatlós,[8] J. M. Deaven,[3,4,5,†] C. J. Guess,[3,4,5,‡] J. Gulyás,[8] K. Hatanaka,[6] K. Hirota,[6] D. Ishikawa,[6] A. Krasznahorkay,[8] H. Matsubara,[6,§] R. Meharchand,[3,4,5,∥] F. Molina,[9,¶] H. Okamura,[6,**] H. J. Ong,[6] G. Perdikakis,[3,4,5,††] C. Scholl,[10,‡‡] Y. Shimbara,[11,§§] G. Susoy,[12] T. Suzuki,[6] A. Tamii,[6] J. H. Thies,[13] and J. Zenihiro[6,∥∥]

^{40}Ar -> ^{40}K

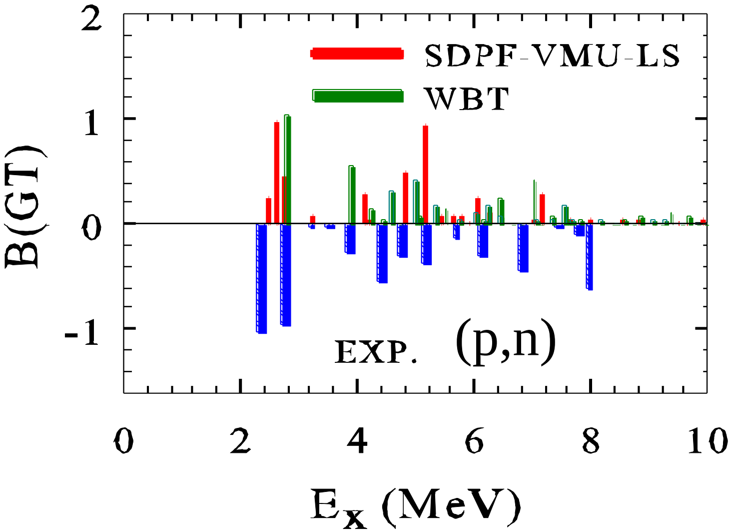

$$R = \frac{B(GT)_{2730\ \text{keV}}}{B(GT)_{2290\ \text{keV}}}.$$

R=0.48

TABLE I. Experimental and shell-model B(GT) values and their ratios for the transitions to the 1^+ states at 2290 and 2730 keV.

$E_x(^{40}$K) (keV)	$B(GT)_{exp}$			$B(GT)_{SM}$[d]	
Ref. [15]	(p,n)[a]	$\beta(^{40}$Ti)[b]	(^{3}He, t)[c]	^{40}Ar→^{40}K	^{40}Ti→^{40}Sc
2289.87(1)	1.03(10)	0.57(3)	—	0.97	0.40
2730.37(2)	0.94(9)	0.94(4)	—	0.42	0.94
R	0.911(5)	1.65(11)	0.73(5)	0.43	2.35

[a]From Ref. [10].
[b]From Ref. [9] and using isospin symmetry.
[c]Only the relative strengths for the two states are known experimentally.
[d]The shell-model calculations have been multiplied by a factor 0.60 to account for quenching of the GT strength [16].

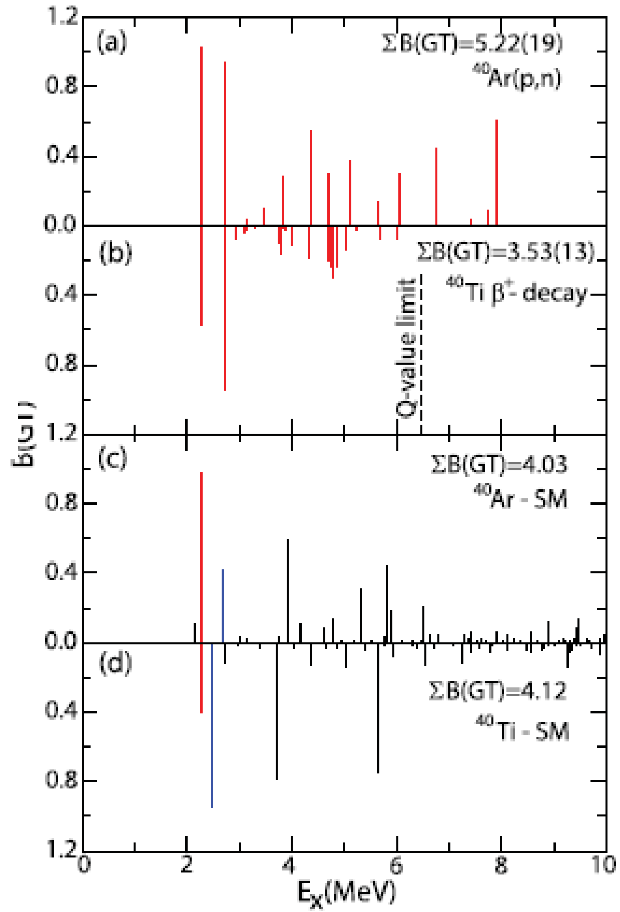

FIG. 1. (Color online) GT strength distributions in the $A = 40$, $T = 2$ isoquintet. (a) Extracted from ^{40}Ar(p,n) [10]. (b) Extracted from β^+ decay of ^{40}Ti. The dashed line indicates the limit of the Q-value window available for β^+ decay. (c) Shell-model calculations for transitions from ^{40}Ar to ^{40}K. (d) Shell-model calculations for transitions from ^{40}Ti to ^{40}Sc.

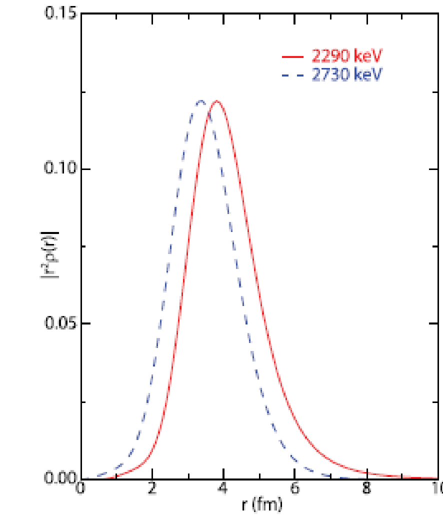

FIG. 3. (Color online) Radial transition densities (multiplied by r^2) for the transitions from ^{40}Ar to the 1^+ states at 2290 and 2730 keV. The vertical scales have been arbitrarily adjusted so that the peak values of the curves are equal.

WBMB-C

Neutral-current

^{40}Ar

M1

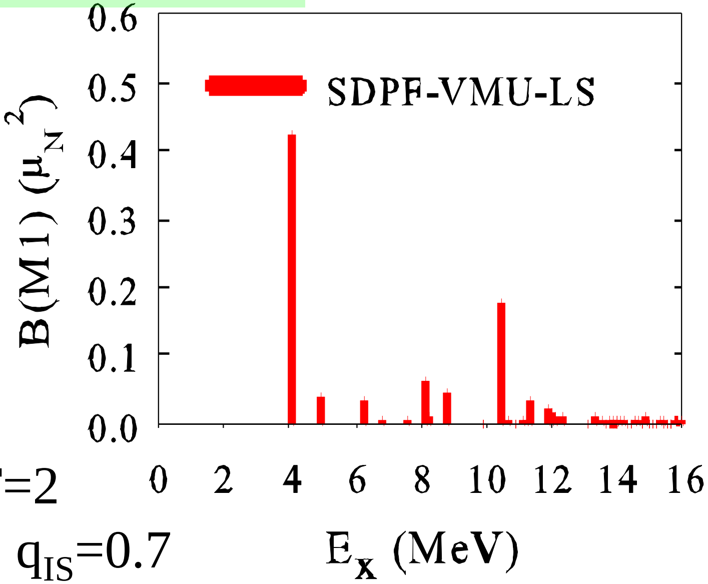

T=2 → T=2

q_{IV}=0.35 q_{IS}=0.7

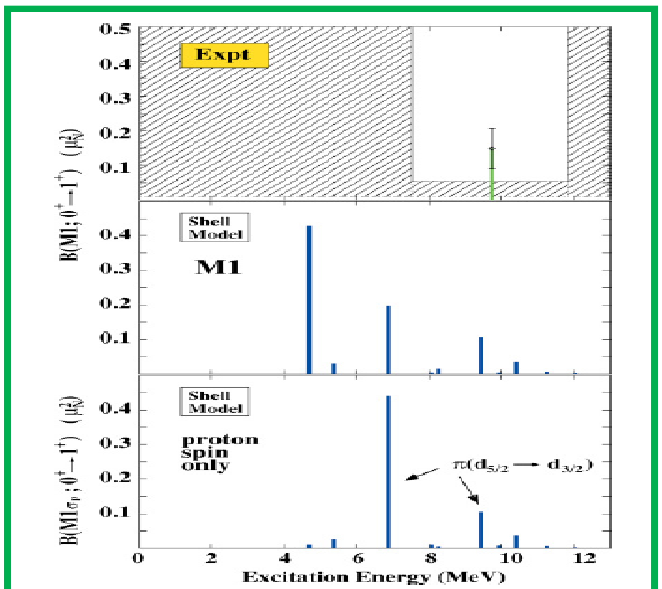

Exp. B(M1)=0.148(59) μ_N^2

Li et al, PR C73, 054306 (2006)

^{40}Ar -> ^{40}K

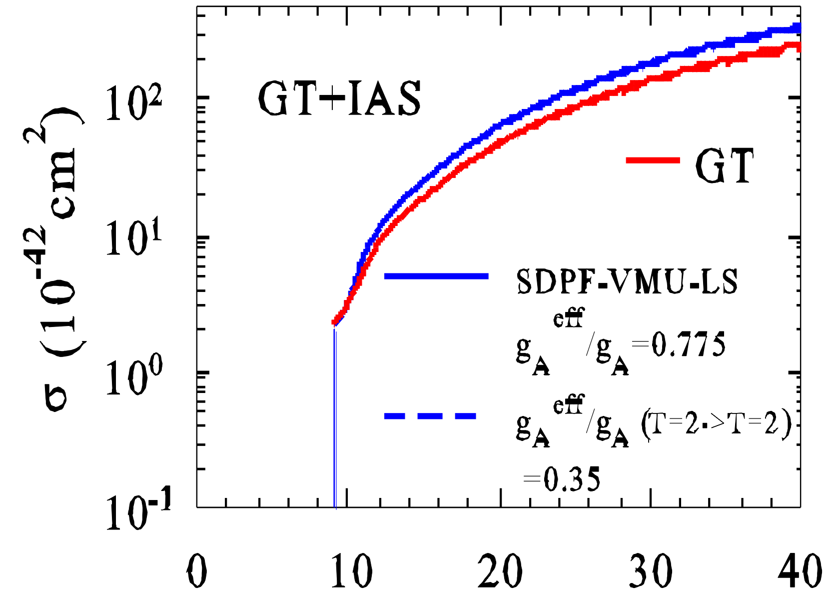

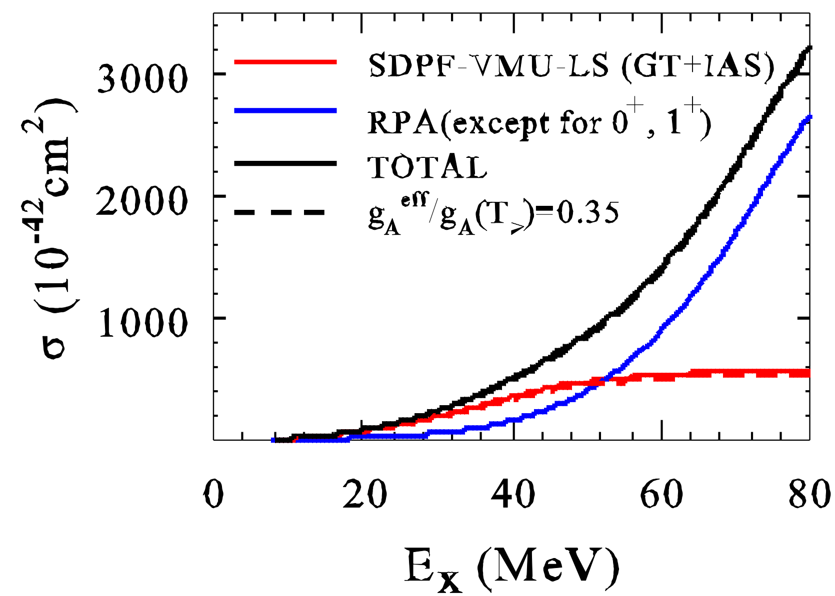

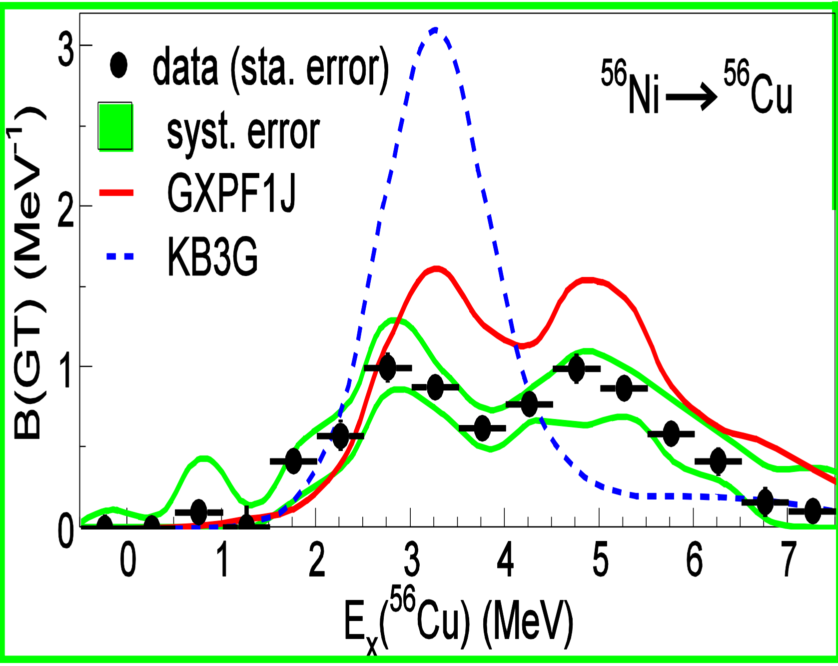

Sasano et al., PRL 107, 202501 (2011)

▪ e-capture rates on ^{56}Ni in stellar environments: $\rho Y_e = 10^7 - 10^{10}\ g/cm^3$

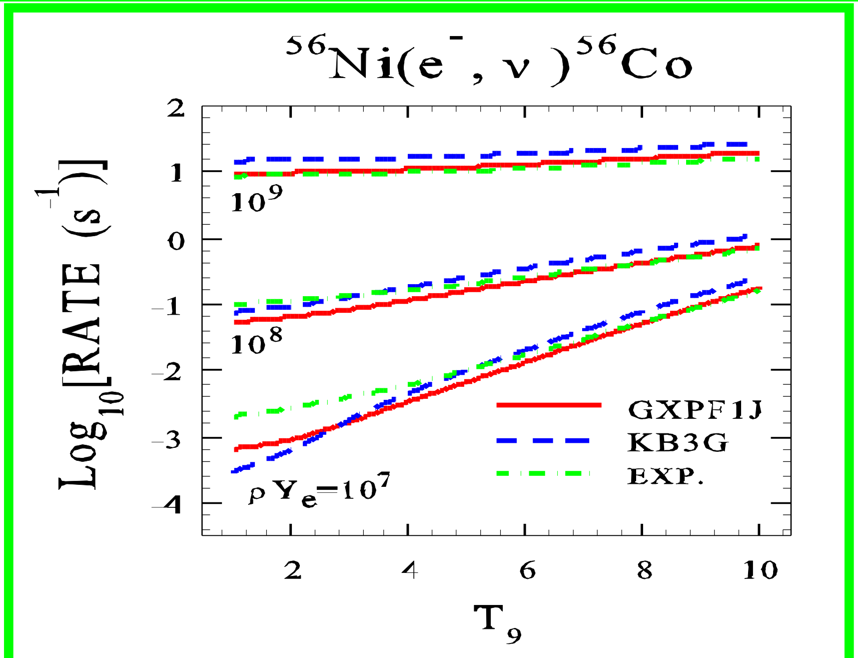

Suzuki, Honma, Mao, Otsuka, Kajino, PR C83, 044619 (2011)

Type-Ia supernova explosion

Accretion of matter to white-dwarf from binary star

→ supernova explosion when white-dwarf mass > Chandrasekhar limit

→ ^{56}Ni (N=Z)

→ $^{56}Ni(e^-, \nu)\,^{56}Co$ $\quad Y_e = 0.5 \rightarrow Y_e < 0.5$ (neutron-rich)

→ production of neutron-rich isotopes; more ^{58}Ni

Decrease of e-capture rate on ^{56}Ni

→ less production of ^{58}Ni.

e-capture rates:
GXPF1J < KB3G
←→
Y_e (GXPF1J) > Y_e (KB3G)

Problem of over-production of ^{58}Ni may be solved.

Problem of over-production of ^{58}Ni

The Astrophysical Journal Supplement Series, 125:439–462, December

NUCLEOSYNTHESIS IN CHANDRASEKHAR MASS MODELS FOR TYPE Ia SUPERNOVAE AND CONSTRAINTS ON PROGENITOR SYSTEMS AND BURNING-FRONT PROPAGATION

Koichi Iwamoto,[1,2,3] Franziska Brachwitz,[4] Ken'ichi Nomoto,[1,2,3] Nobuhiro Kishimoto,[1]
Hideyuki Umeda,[2,3] W. Raphael Hix,[3,5] and Friedrich-Karl Thielemann[3,4,5]

Received 1999 January 11 ; accepted 1999 July 29

and ignition densities to put new constraints on the above key quantities. The abundance of the Fe group, in particular of neutron-rich species like ^{48}Ca, ^{50}Ti, ^{54}Cr, ^{54,58}Fe, and ^{58}Ni, is highly sensitive to the electron captures taking place in the central layers. The yields obtained from such a slow central

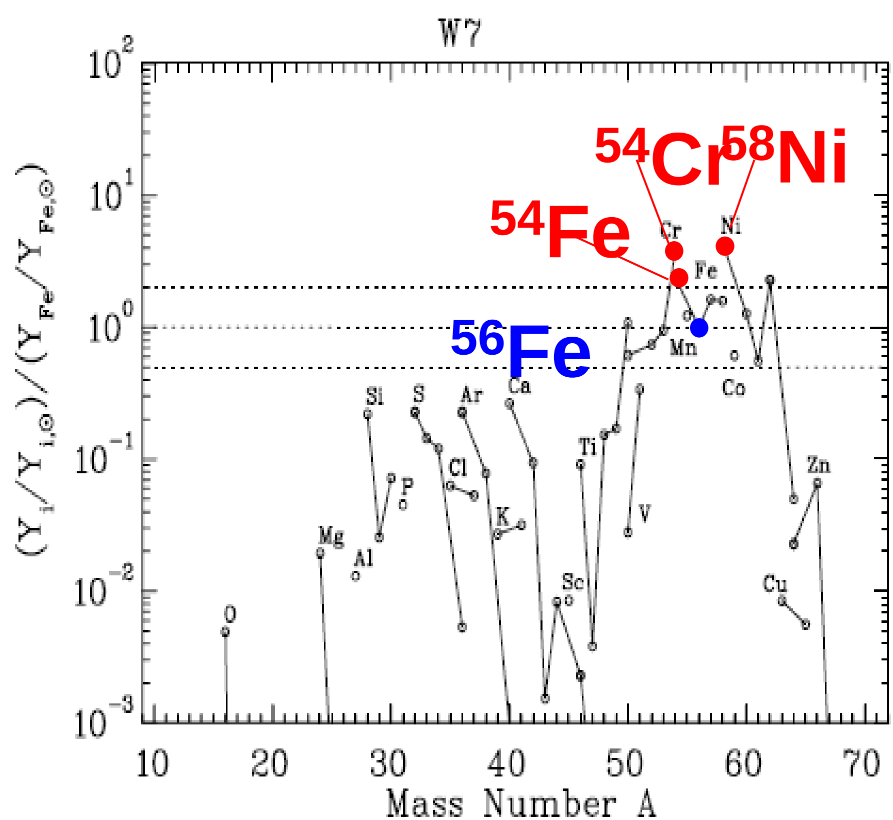

Famiano

NSE(Nuclear Statistical Equilibrium) calculation

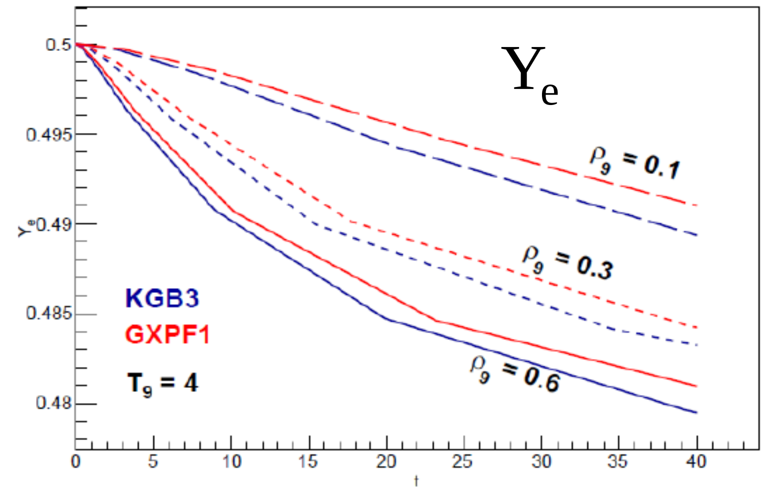

Ratio between ^{58}Ni / ^{56}Ni

GXPF1 -> ^{58}Ni/^{56}Ni decreases

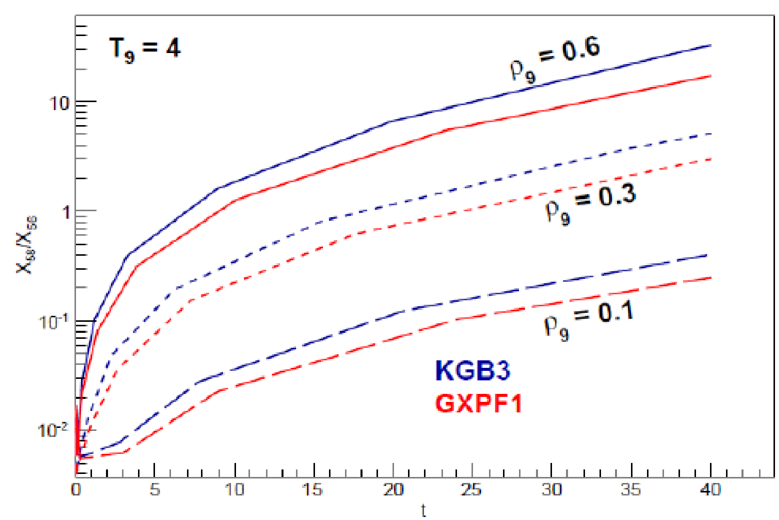

●Neutral current reaction on ^{56}Ni

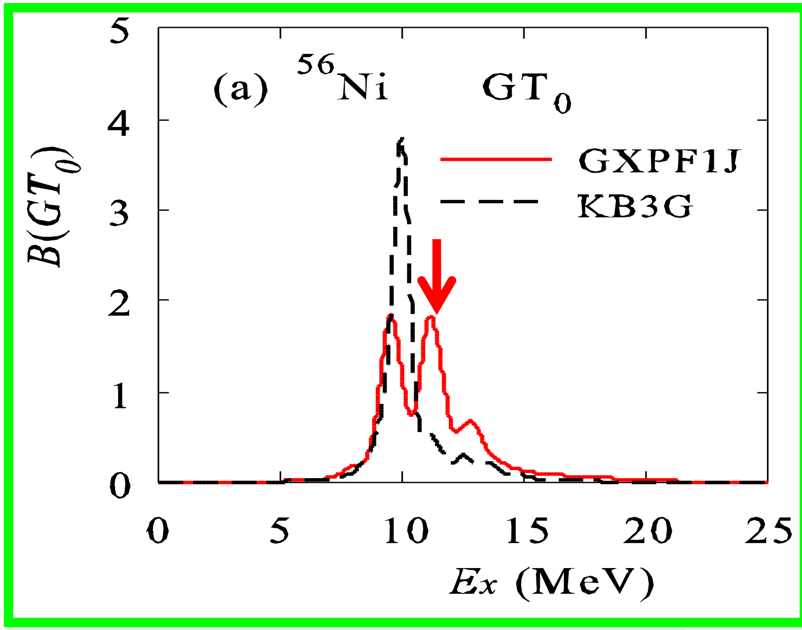

B(GT)=6.2 (GXPF1J)
B(GT)=5.4 (KB3G)

p-emission BR increses

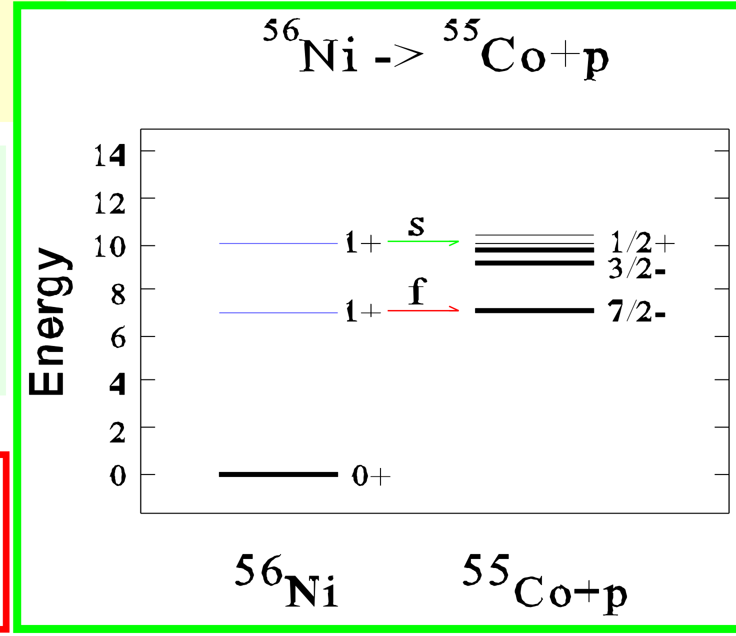

Synthesis of Mn in Population III Star

$^{56}Ni(\nu,\nu' p)^{55}Co, \quad ^{55}Co(e^-,\nu)^{55}Fe(e^-,\nu)^{55}Mn$

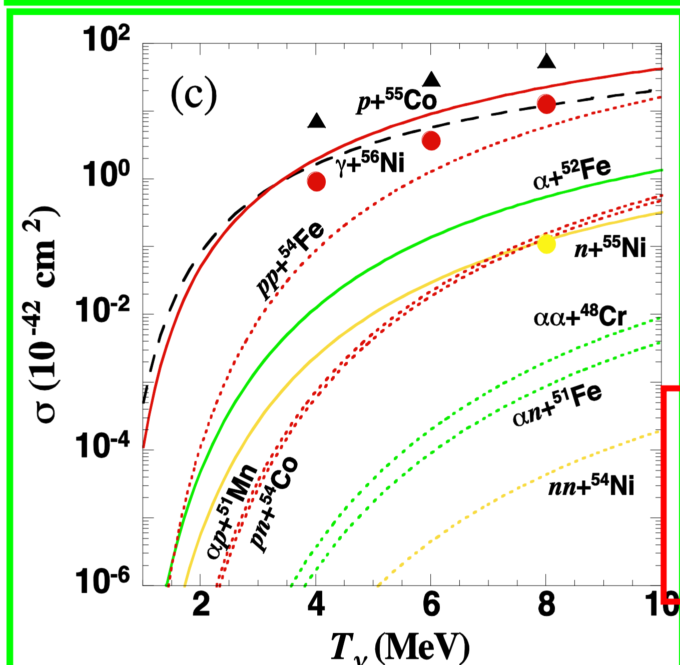

cf: HW02

▲ gamma
● p
● n

p-emission x-sections increse

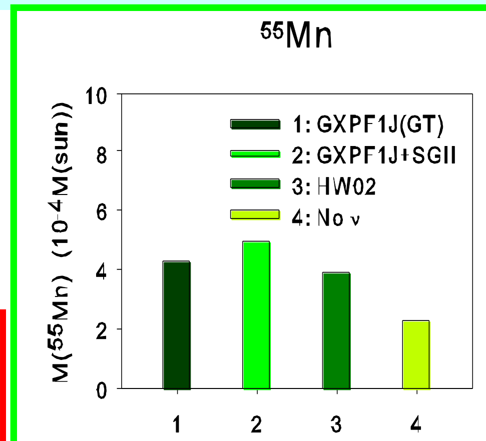

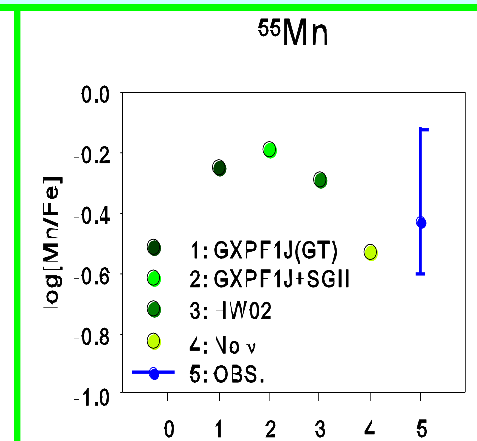

$^{54}Fe(p,\gamma)^{55}Co$

Yoshida, Umeda, Nomoto

rp-process and X-ray burst

(p, γ) & β^+-decay/e-capture

→ ^{50}Fe(,e$^+\nu$)^{50}Mn ^{50}Fe(e$^-$,ν)^{50}Mn

→ ^{55}Ni(e$^-$,ν)^{55}Co

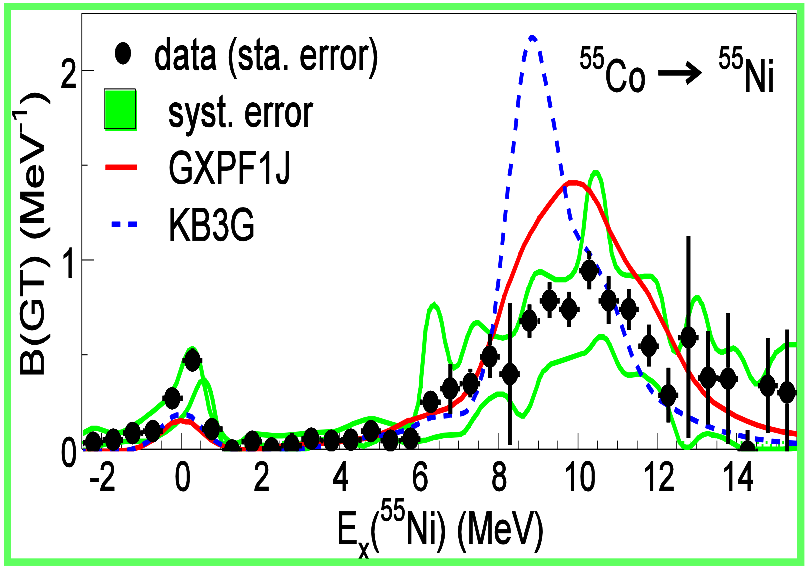

Sasano et al.

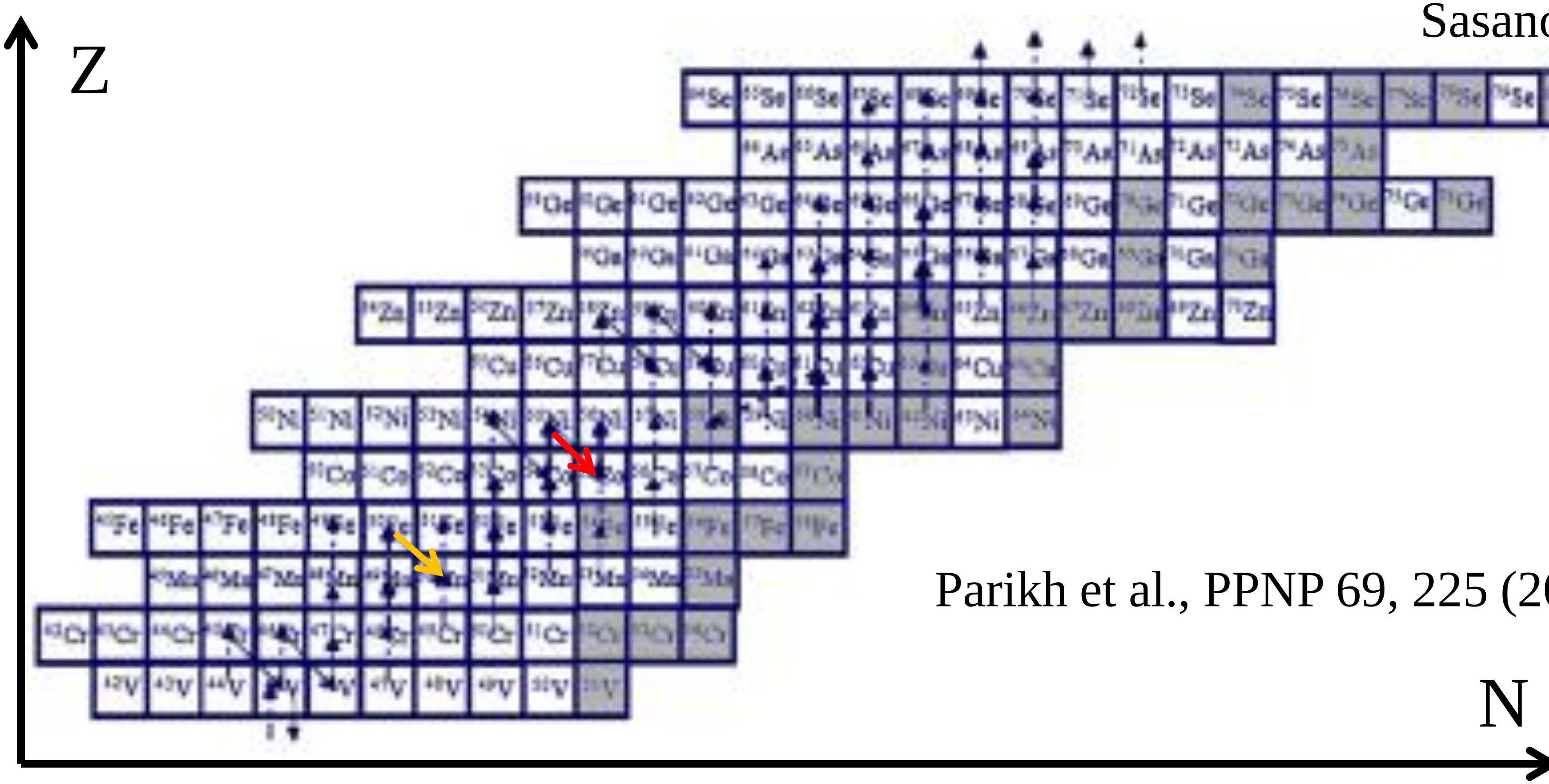

Parikh et al., PPNP 69, 225 (2013)

X-ray burst

GXP_rp.mov KBF_rp.mov

e-capture and beta-decay rates with KBF:
Langanke and Martinez-Pinedo, Atomic Data and Nuclear Data Tables **79,** 1 (2001)

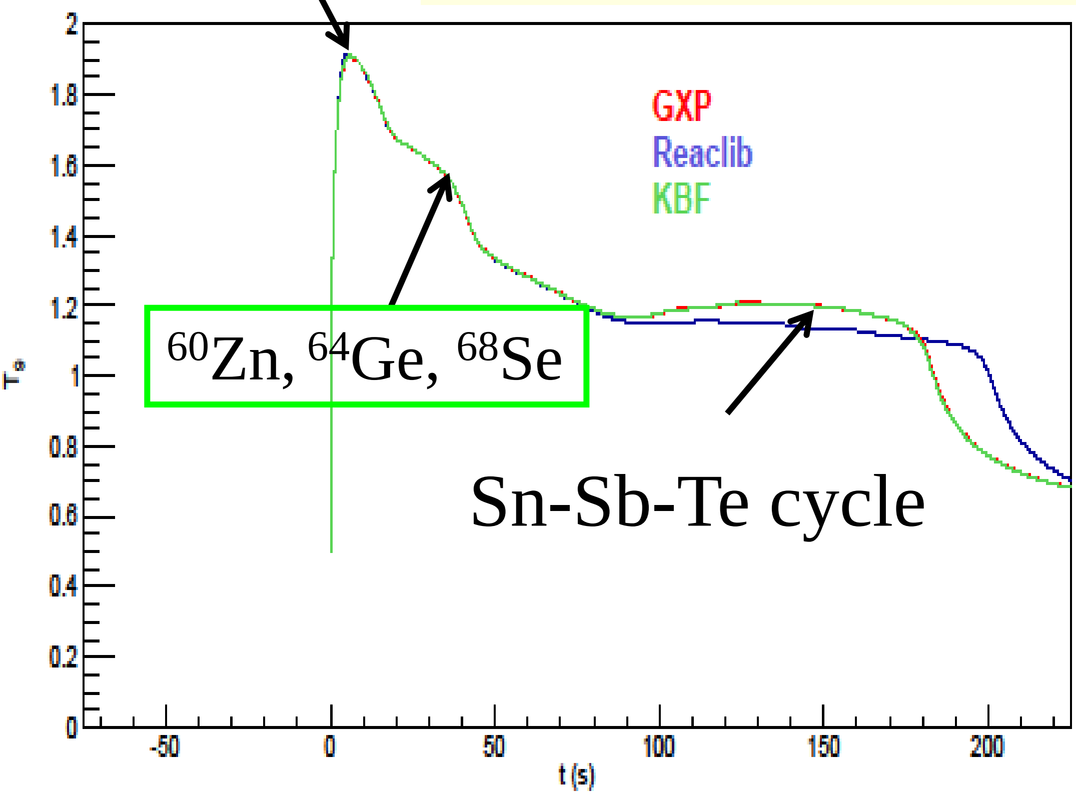

Famiano

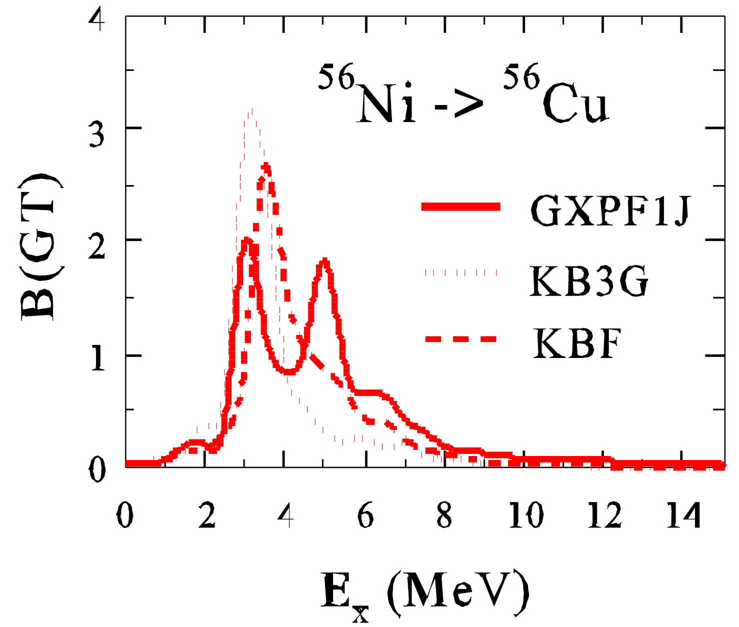

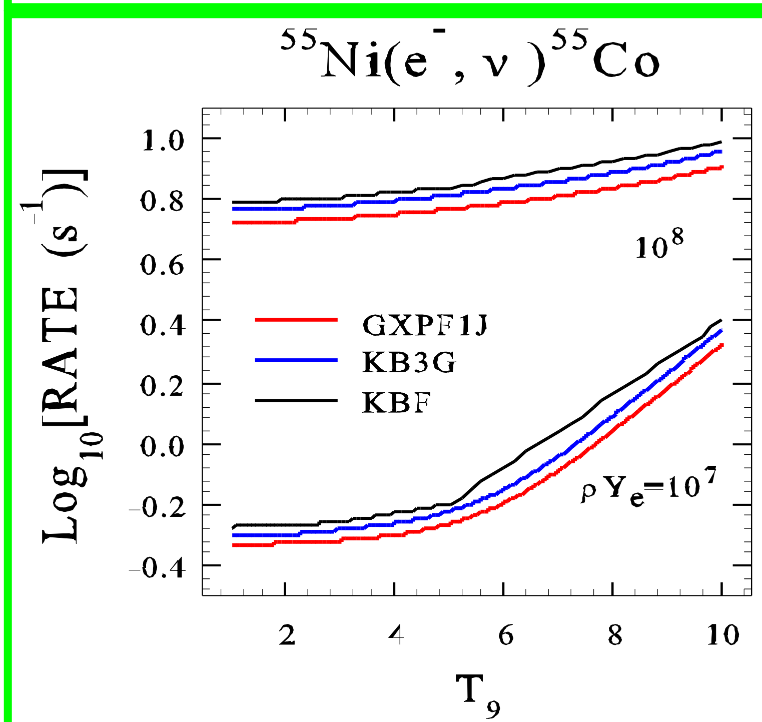

Electron-capture and β-decay rates at stellar environments

○Evolution of 8-10$M_\odot$ stars and nuclear URCA processes

- $M=0.5 \sim 8M_\odot$: He burning → C-O core → C-O white dwarfs
- $M > 10M_\odot$: → Fe core → core-collapse supernova explosion
- $M=8M_\odot \sim 10M_\odot$: C burning → O-Ne-Mg core
  - → (1) O-Ne-Mg white dwarf (WD)
  - → (2) e-capture supernova explosion (collapse of O-Ne-Mg core induced by e-capture) with neutron star (NS) remnant
  - → (3) core-collapse (iron-core collapse) supernova explosion with NS (neon burning shell propagates to the center)

Fate of the star is sensitive to its mass and nuclear e-capture and β–decay rates; Cooling of O-Ne-Mg core by nuclear URCA processes determines (2) or (3).

Nomoto and Hashimoto, Phys. Rep. 163, 13 (1988)
Miyaji, Nomoto, Yokoi, and Sugimoto, Pub. Astron. Soc. Jpn. 32, 303 (1980)
Nomoto, Astrophys. J. 277, 791 (1984); ibid. 322, 206 (1987)

▪Detailed e-capture and beta-decay rates for URCA nuclear pairs in 8-10 solar-mass stars

Nuclear URCA process

$$^{23}Na + e^{-} \rightarrow {}^{23}Ne + \nu$$

$$^{23}Ne \rightarrow {}^{23}Na + e^{-} + \bar{\nu}$$

$$^{25}Mg + e^{-} \rightarrow {}^{25}Na + \nu$$

$$^{25}Na \rightarrow {}^{25}Mg + e^{-} + \bar{\nu}$$

$$^{27}Al + e^{-} \rightarrow {}^{27}Mg + \nu$$

$$^{27}Mg \rightarrow {}^{27}Al + e^{-} + \bar{\nu}$$

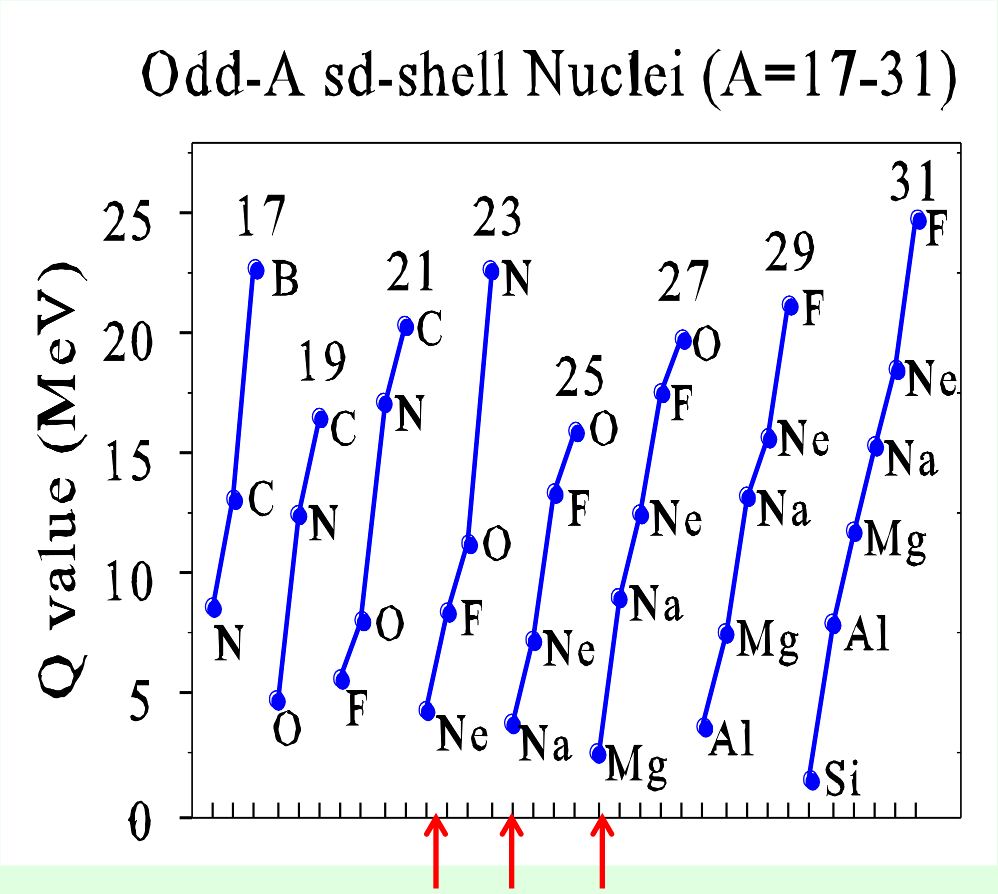

Cooling of O-Ne-Mg core of stars

→ ‘e-cap.SNe’ or ‘core-collapse SNe’

sd-shell: USDB Brown and Richter, PR C74, 034315 (2006)

Richter, Mkhize, Brown, PR C78, 064302 (2008)

(^{23}Ne, ^{23}Na)

PHYSICAL REVIEW C 88, 015806 (2013)

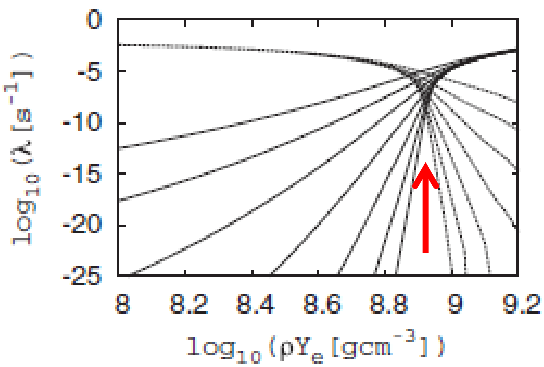

FIG. 2. β-transition rates for the $A = 23$ URCA nuclear pair (^{23}Ne, ^{23}Na) for various temperatures as functions of density $\log_{10} \rho Y_e$. β-decay rates (dashed lines) are those decreasing with density, while electron-capture rates (solid lines) are those increasing with density. The temperature steps are shown in the range of $\log_{10} T = 8$ to 9.2 in steps of 0.2.

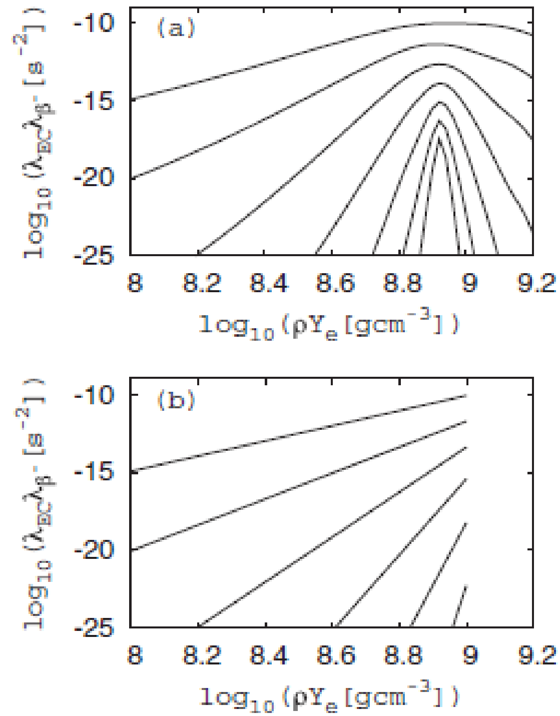

FIG. 3. Product of β-transition rates for the $A = 23$ URCA nuclear pair (^{23}Ne, ^{23}Na) for various temperatures as functions of density $\log_{10} \rho Y_e$. In panel (a), the mesh points are taken from $\log_{10} \rho Y_e = 8.0$ to 9.2 in steps of 0.02, while in panel (b), they are from $\log_{10} \rho Y_e = 8.0$ to 9.0 in a single step as in Oda *et al.* [10].

$\Delta \log_{10}(\rho Y_e) = 0.06$

$\Delta \log_{10}(\rho Y_e) = 0.2$

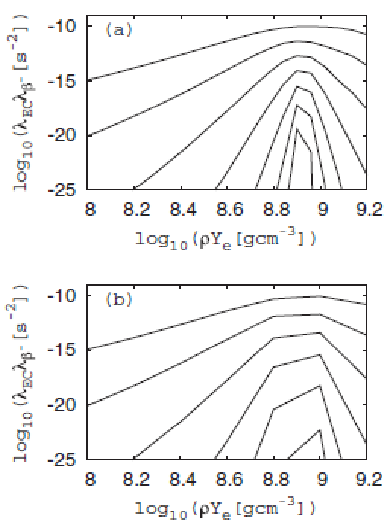

$8.0 < \log_{10}(\rho Y_e) < 9.2$ in steps of 0.02

$8.0 < \log_{10} T < 9.2$ in steps of 0.05

cf: Oda et al., At. Data and Nucl. Data Tables 56, 231 (1994): $\Delta \log_{10}(\rho Y_e) = 1.0$

URCA density at $\log_{10} \rho Y_e = 8.92$ for $A = 23$

(^{25}Na, ^{25}Mg)

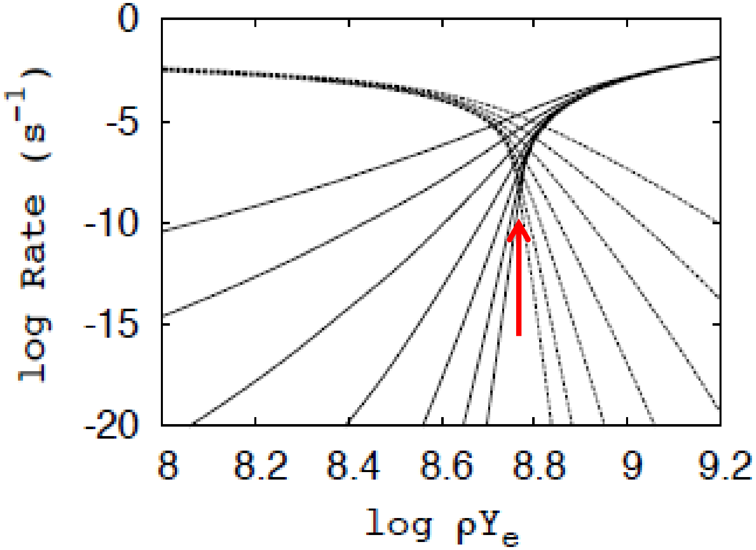

URCA density at $\log_{10} \rho Y_e = 8.78$

(^{27}Mg, ^{27}Al) g.s. $1/2^+$&$5/2^+$

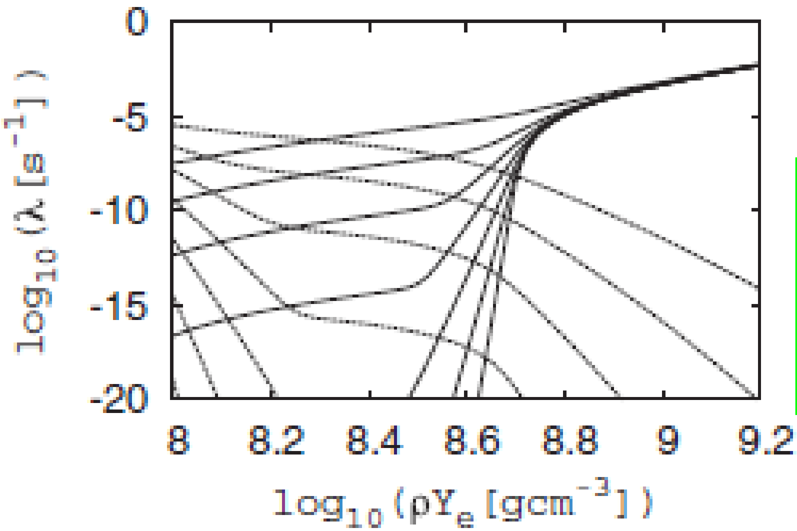

No clear URCA density for A=27

Cooling of O-Ne-Mg core by the nuclear URCA processes

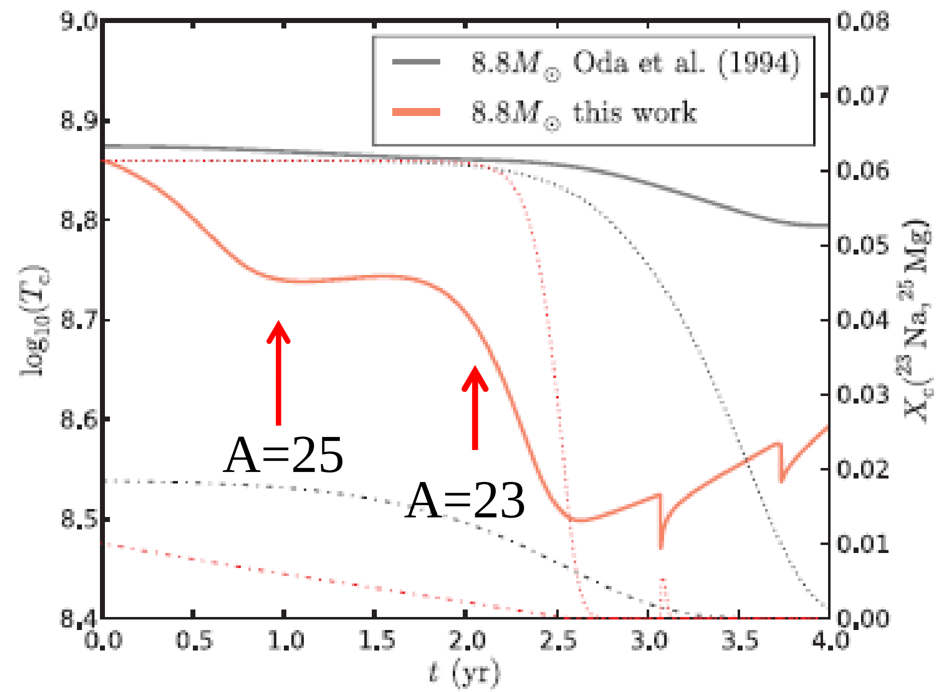

8.8$M_\odot$ star collapses triggered by subsequent e-capture on ^{24}Mg and ^{20}Ne (e-capture supernova explosion)

Toki, Suzuki, Nomoto, Jones and Hirschi, PR C 88, 015806 (2013)
Jones et al., Astrophys. J. 772, 150 (2013)

Energy generation and ν cooling

$$< E_{prod} > = \mu_e - Q_{nucl} - < E_\nu > \qquad kT\frac{ds}{dt} = \frac{dY_e}{dt} < E_{prod} >$$

$$Q_{nucl} = M_d c^2 - M_p c^2,$$

$$< E_{prod} > = Q_{nucl} - \mu_e - < E_\nu >$$

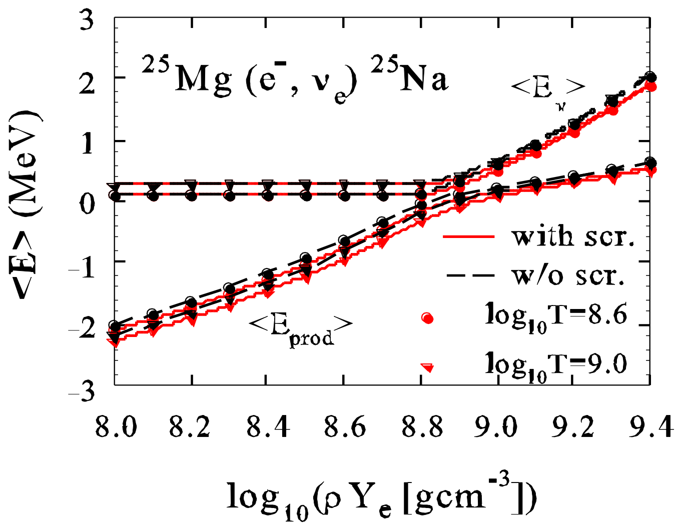

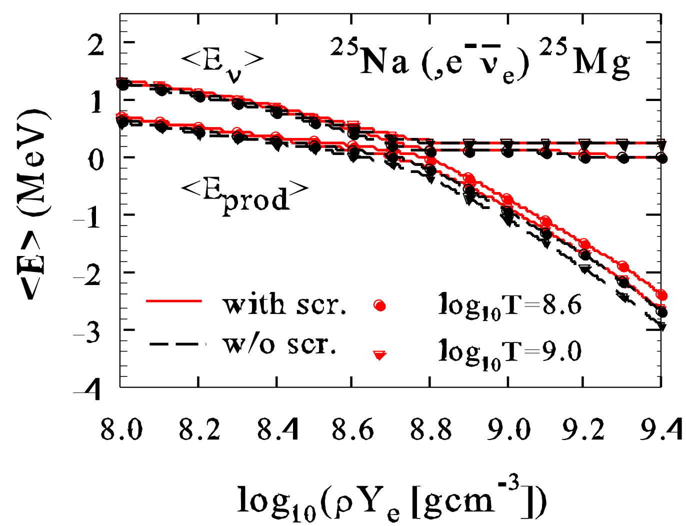

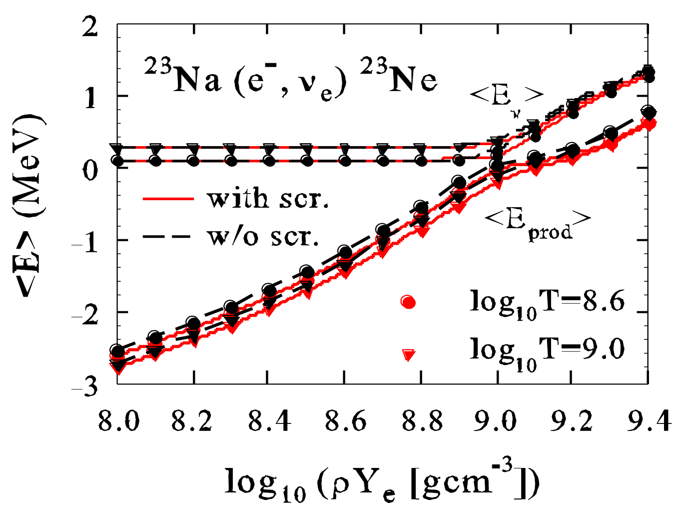

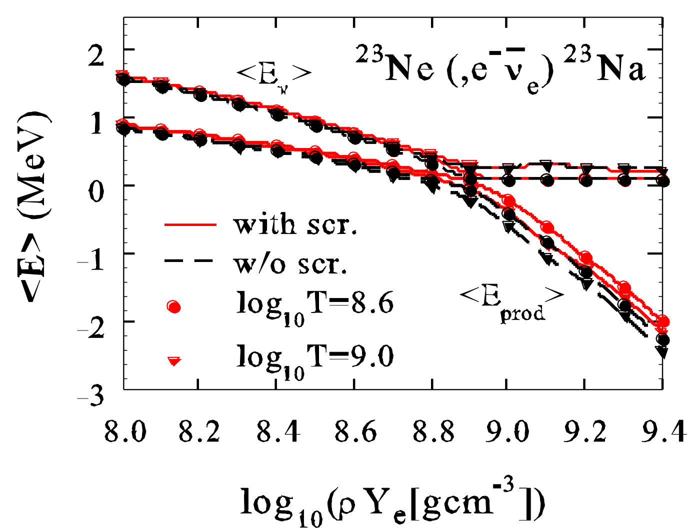

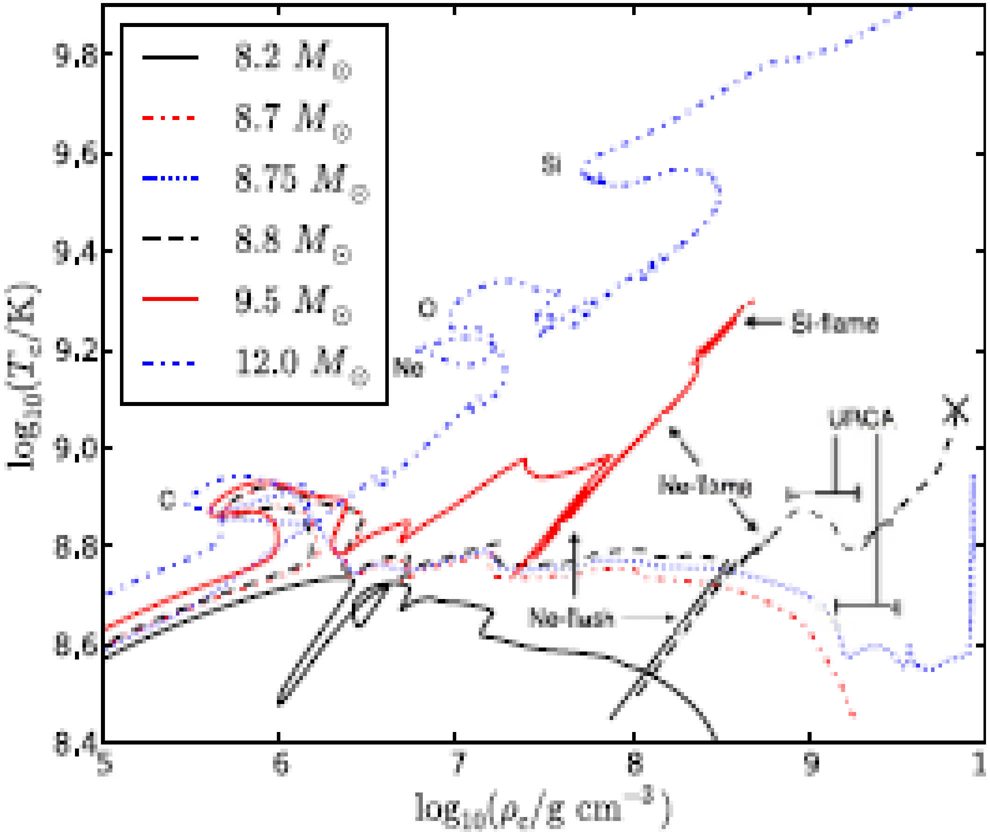

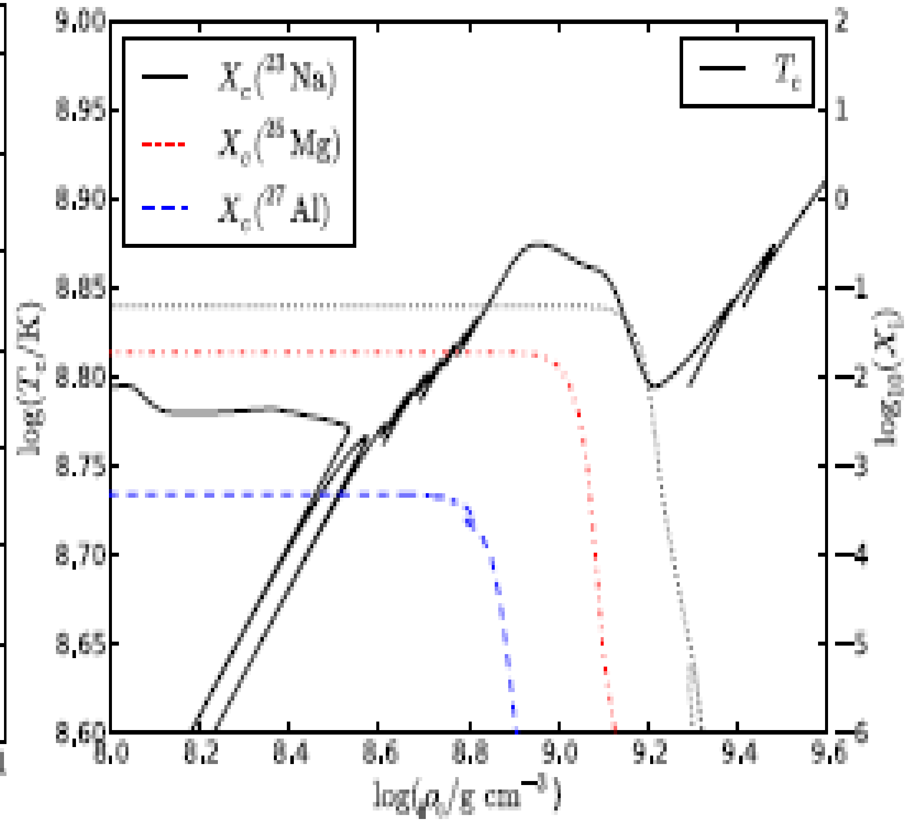

Summary of Model Properties

	8.2 $M_\odot$	8.7 $M_\odot$	8.75 $M_\odot$	8.8 $M_\odot$	9.5 $M_\odot$	12.0 $M_\odot$
Remnant	ONe WD	ONe WD/NS	NS	NS	NS	NS
SN type	...	.../EC-SN (IIP)	EC-SN (IIP)	EC-SN (IIP)	CC-SN (IIP)	CC-SN (IIP)

Jones et al., Astrophys. J. 772, 150 (2013)

Coulomb corrections: screening effects

1. Screening effects of electrons

$V(r)$ with screening effects of relativistic degenerate electron liquid

$$V(r) = -\frac{Ze^2}{2\pi^2}\int \frac{e^{i\vec{k}\vec{r}}}{k^2\epsilon(k,0)}d^3k = -\frac{Ze^2 2k_F}{2k_F r}\frac{2}{\pi}\int \frac{\sin(2k_F q r)}{q^2\epsilon(q,0)}dq.$$

$$V_s(r) = V(r) - \left(-\frac{Ze^2}{r}\right) = Ze^2(2k_F)J,$$

Juodagalvis et al., Nucl. Phys. A 848, 454 (2010).
Itoh et al, Astrophys. J. 579, 380 (2002).

Vs(0)>0 → reduce (enhance) e-capure (β-decay) rates

2. Change of threshold energy

$$\Delta Q_C = \mu_C(Z-1) - \mu_C(Z),$$

$\mu_C(Z)$ =the correction of the chemical potential of the ion with Z

ΔQ_c → reduce e-capture rates & enhance β-decay rates

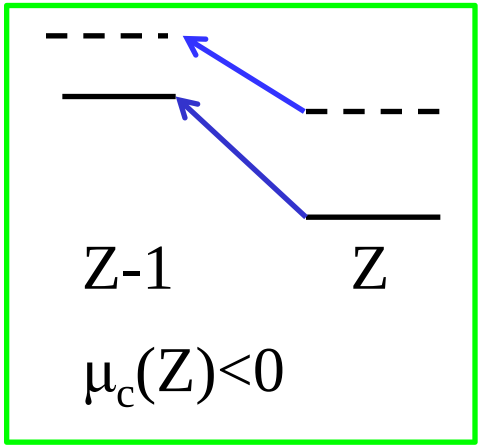

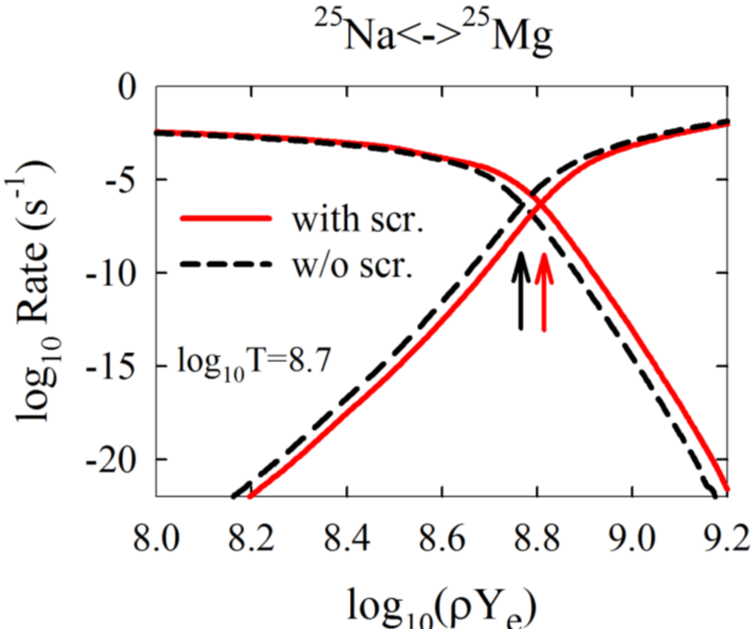

Slattery, Doolen, DeWitt, Phys. Rev. A26, 2255 (1982).
Ichimaru, Rev. Mod. Phys. 65, 255 (1993).

$$\rho Y_e = 8.78 \rightarrow 8.81$$

URCA density → higher density region

Even-A sd-shell Nuclei (A=18-30)

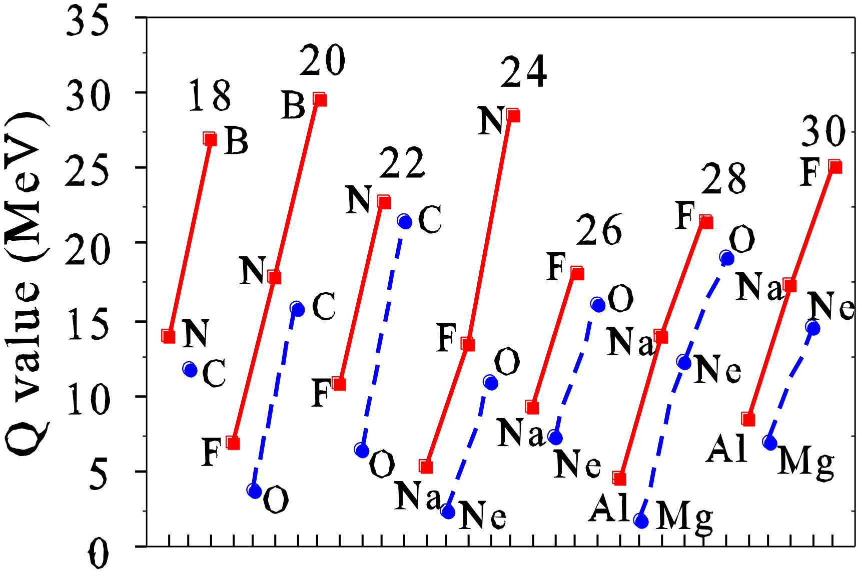

Odd-A sd-shell Nuclei (A=17-31)

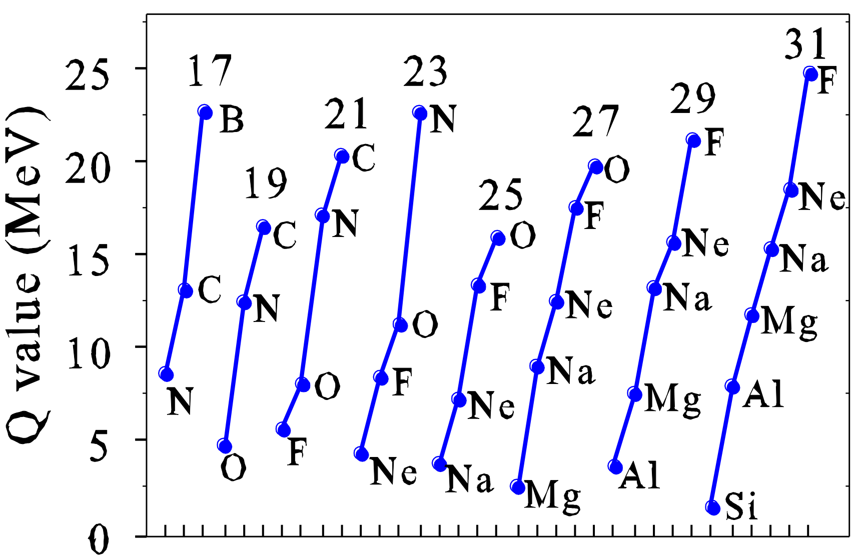

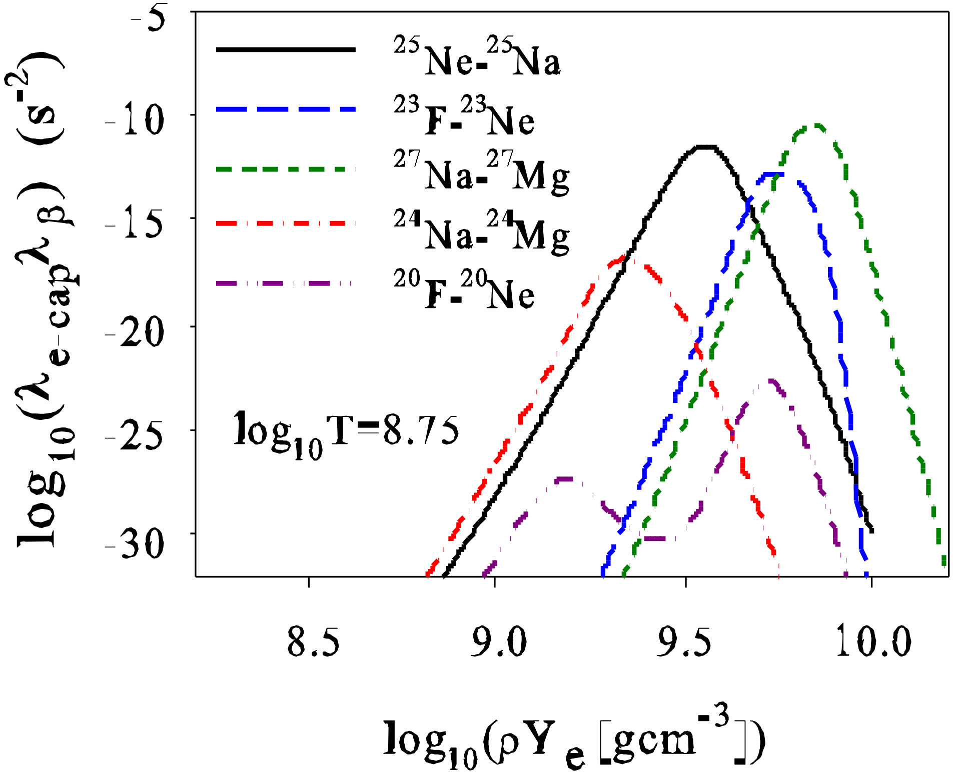

$^{24}Mg(e^-,\nu_e)^{24}Na(e^-,\nu_e)^{24}Ne$

$^{20}Ne(e^-,\nu_e)^{20}F(e^-,\nu_e)^{20}O$

Heating of stars

Suzuki, Toki and Nomoto, submitted to Ast. J.

LETTER

Nature 505, 65 (2014)

doi:10.1038/nature12757

Strong neutrino cooling by cycles of electron capture and β^- decay in neutron star crusts

H. Schatz[1,2,3], S. Gupta[4], P. Möller[2,5], M. Beard[2,6], E. F. Brown[1,2,3], A. T. Deibel[2,3], L. R. Gasques[7], W. R. Hix[8,9], L. Keek[1,2,3], R. Lau[1,2,3], A. W. Steiner[2,10] & M. Wiescher[2,6]

Table 1 | Electron-capture/β^--decay pairs with highest cooling rates

Electron-capture/β^--decay pair		Density†	Chemical potential†	Luminosity‡
Parent	Daughter*	(10^{10} g cm^{-3})	(MeV)	(10^{36} erg s^{-1})
^{29}Mg	^{29}Na	4.79	13.3	24
^{55}Ti	^{55}Sc, ^{55}Ca	3.73	12.1	11
^{31}Al	^{31}Mg	3.39	11.8	8.8
^{33}Al	^{33}Mg	5.19	13.4	8.3
56Ti	56Sc	5.57	13.8	3.5
^{57}Cr	^{57}V	1.22	8.3	1.6
^{57}V	^{57}Ti, ^{57}Sc	2.56	10.7	1.6
^{63}Cr	^{63}V	6.82	14.7	0.97
^{105}Zr	^{105}Y	3.12	11.2	0.92
^{59}Mn	^{59}Cr	0.945	7.6	0.88
^{103}Sr	^{103}Rb	5.30	13.3	0.65
^{96}Kr	^{96}Br	6.40	14.3	0.65
^{65}Fe	^{65}Mn	2.34	10.3	0.60
^{65}Mn	^{65}Cr	3.55	11.7	0.46

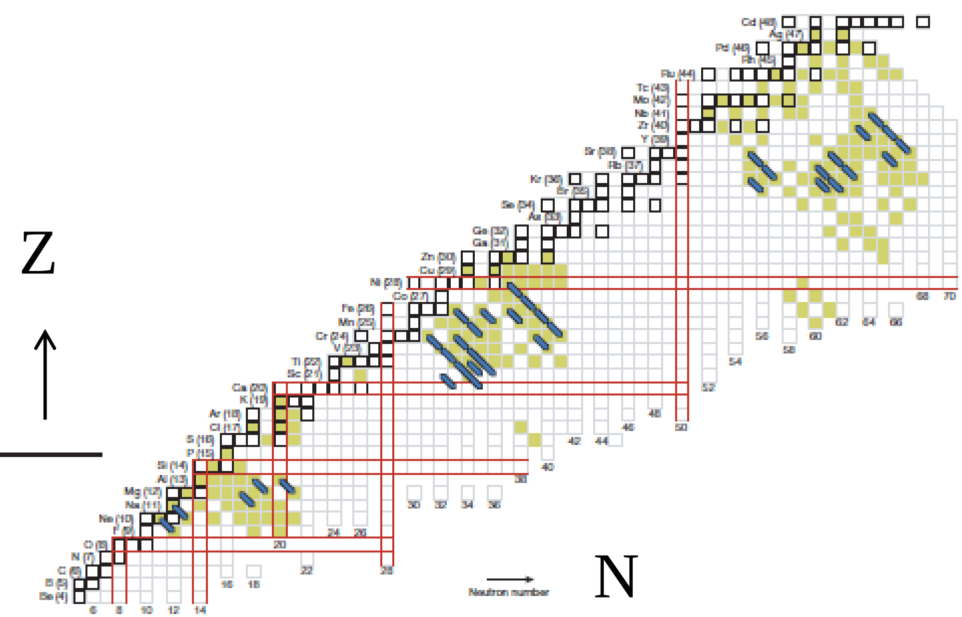

Figure 2 | Electron-capture/β^--decay pairs on a chart of the nuclides. The thick blue lines denote electron-capture/β^--decay pairs that would generate a strong neutrino luminosity in excess of 5×10^{34} erg s^{-1} at $T = 0.51$ GK for a composition consisting entirely of the respective electron-capture/β^--decay pair. They largely coincide with regions where allowed electron-capture and β^--decay transitions are predicted to populate low-lying states and subsequent electron capture is blocked (shaded squares, see also the discussion in ref. 3). These are mostly regions between the closed neutron and proton shells (pairs of horizontal and vertical red lines), where nuclei are significantly deformed (see Supplementary Information section 4). Nuclides that are β^--stable under terrestrial conditions are shown as squares bordered by thicker lines. Nuclear charge numbers are indicated in parentheses next to element symbols.

200el

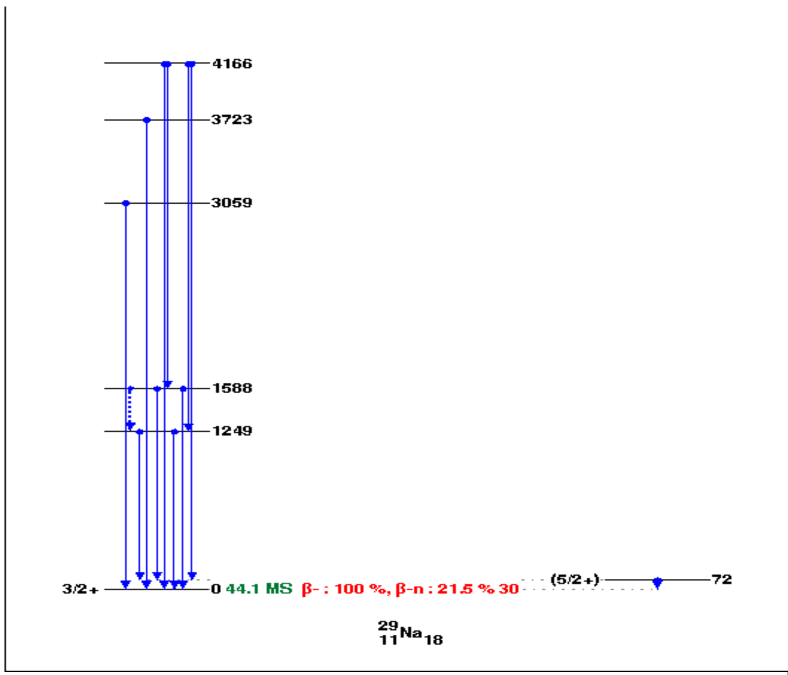

4166
3723
3059
1588
1249
3/2+
0 44.1 MS β- : 100 %, β-n : 21.5 % 30
(5/2+)
72
$^{29}_{11}Na_{18}$

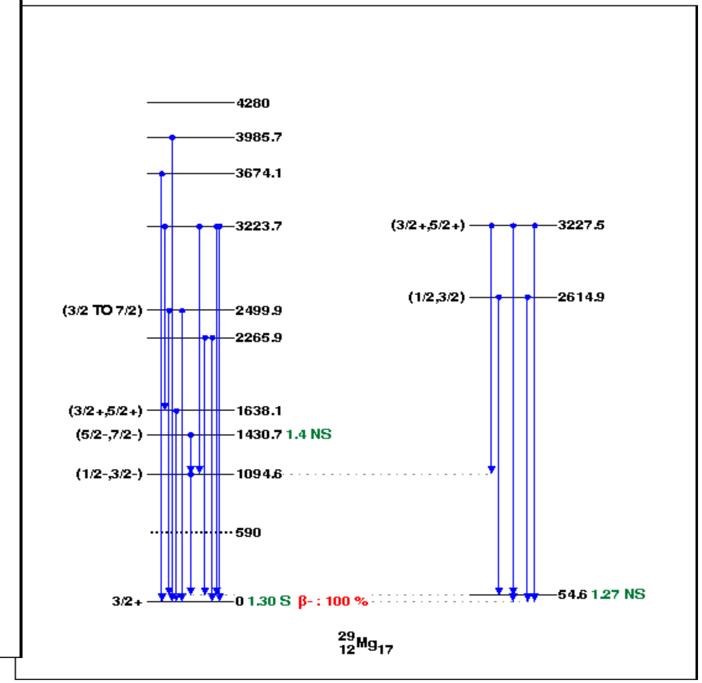

4280
3985.7
3674.1
3223.7
(3/2 TO 7/2) 2499.9
2265.9
(3/2+,5/2+) 1638.1
(5/2-,7/2-) 1430.7 1.4 NS
(1/2-,3/2-) 1094.6
590
3/2+ 0 1.30 S β- : 100 %
(3/2+,5/2+) 3227.5
(1/2,3/2) 2614.9
54.6 1.27 NS
$^{29}_{12}Mg_{17}$

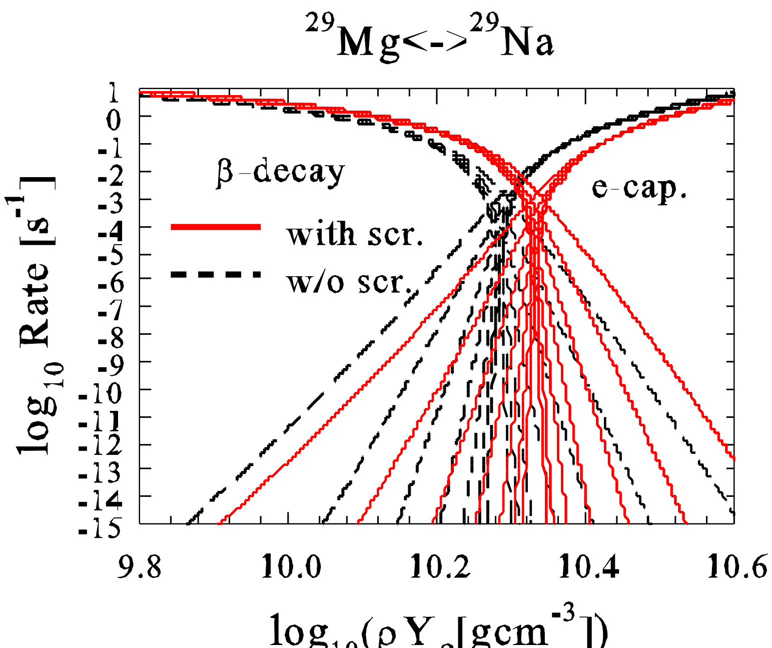

^{29}Mg<->^{29}Na
β-decay
e-cap.
with scr.
w/o scr.
$\log_{10}$ Rate [s^{-1}]
$\log_{10}(\rho Y_e[gcm^{-3}])$

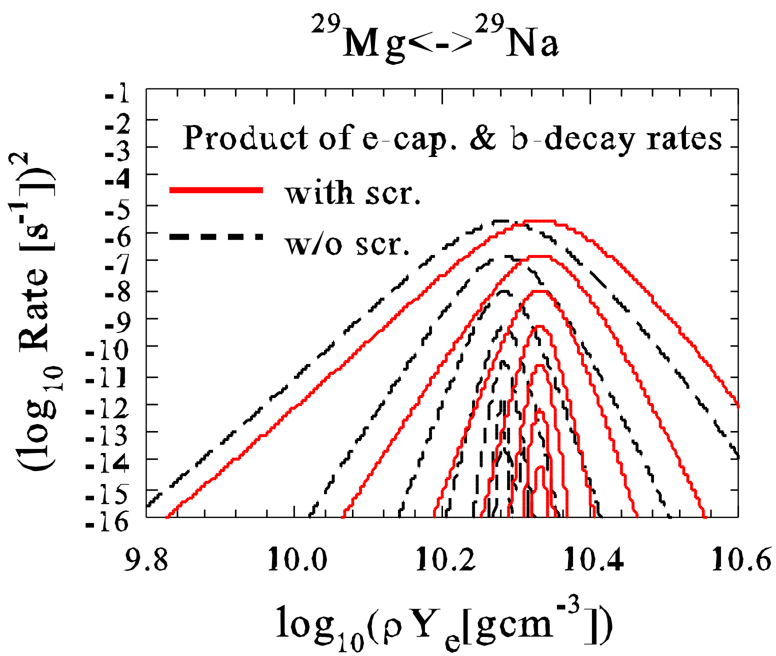

^{29}Mg<->^{29}Na
Product of e-cap. & b-decay rates
with scr.
w/o scr.
$(\log_{10}$ Rate [s^{-1}]$)^2$
$\log_{10}(\rho Y_e[gcm^{-3}])$

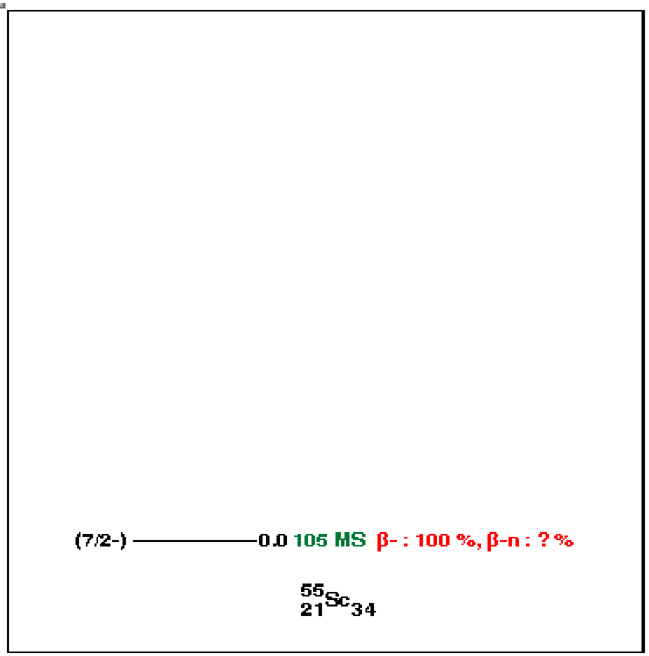

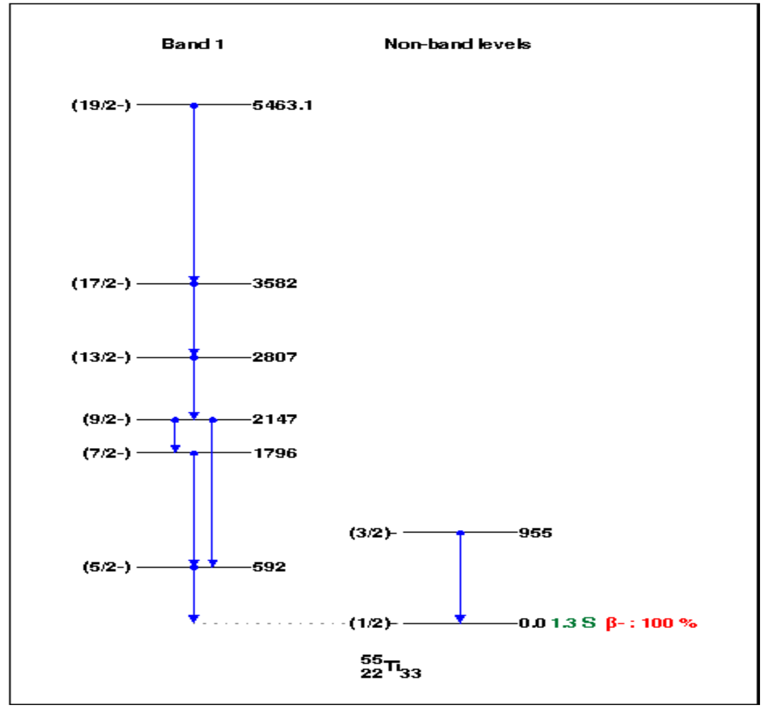

^{55}Ti (1/2$^-$) <-> ^{55}Sc (7/2$^-$)

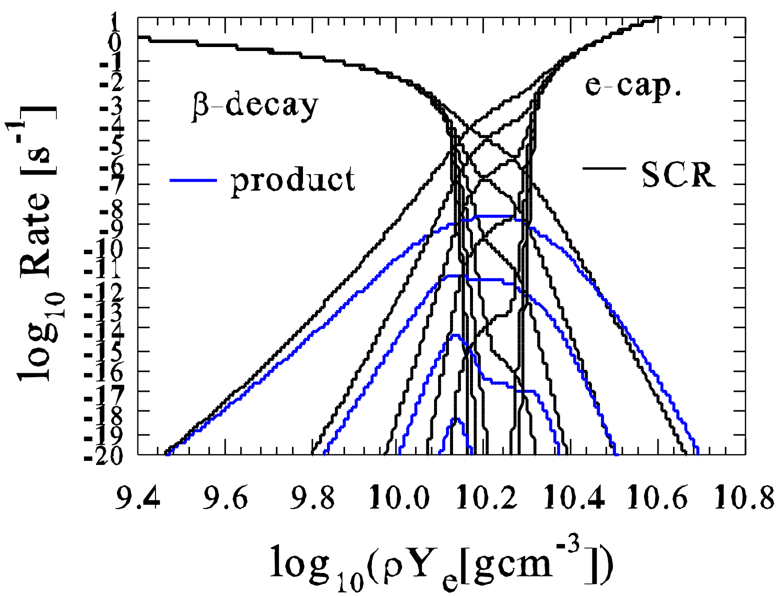

^{55}Ti (1/2$^-$) <-> ^{55}Sc (7/2$^-$)

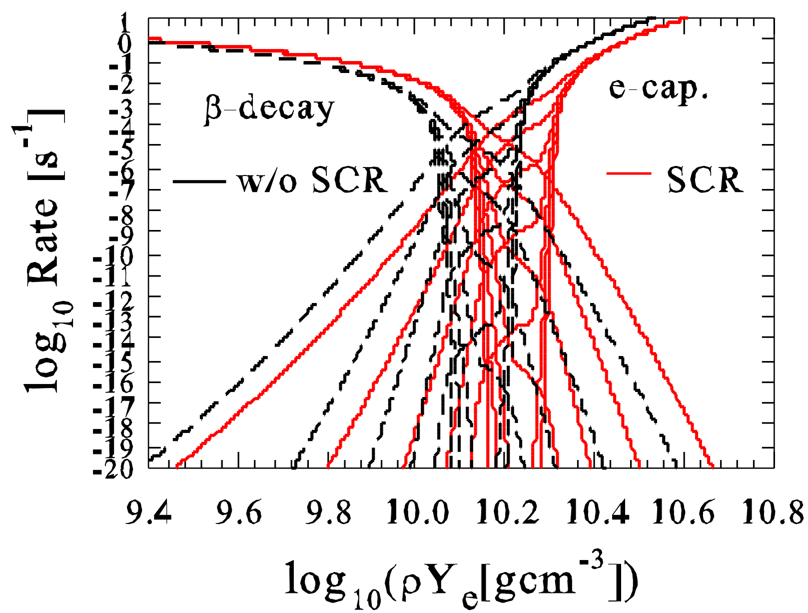

○ Beta-Decays of r-process waiting-point nuclei at N=126

R-process

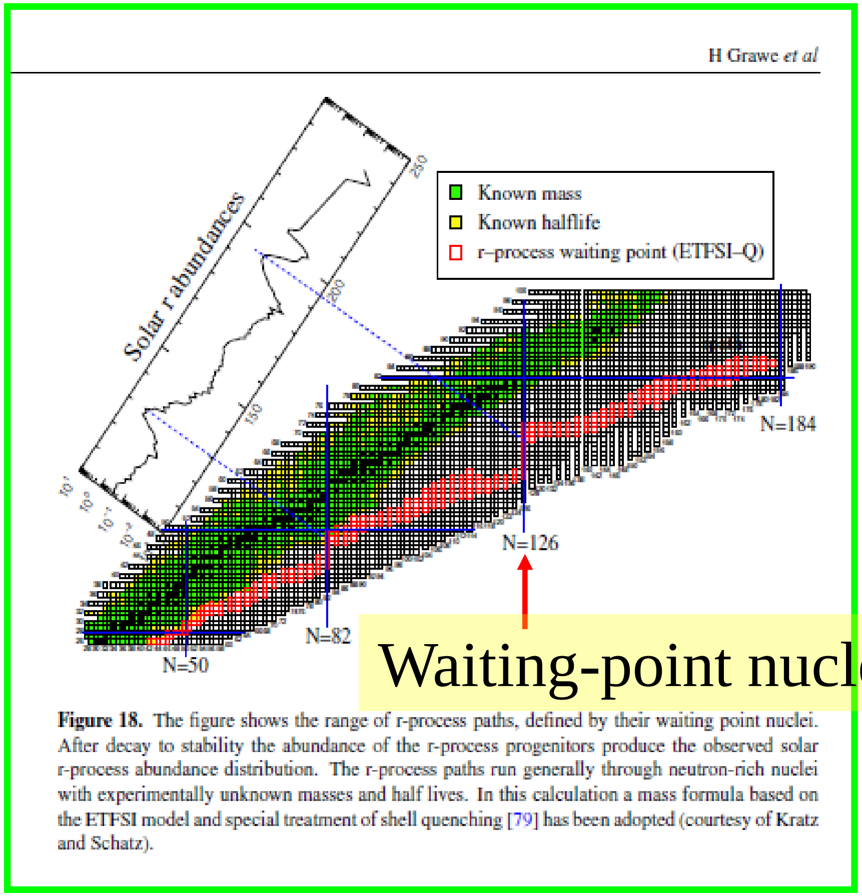

Figure 18. The figure shows the range of r-process paths, defined by their waiting point nuclei. After decay to stability the abundance of the r-process progenitors produce the observed solar r-process abundance distribution. The r-process paths run generally through neutron-rich nuclei with experimentally unknown masses and half lives. In this calculation a mass formula based on the ETFSI model and special treatment of shell quenching [79] has been adopted (courtesy of Kratz and Schatz).

Waiting-point nuclei

Shell Model

Z=64-73

Gamow-Teller strengths

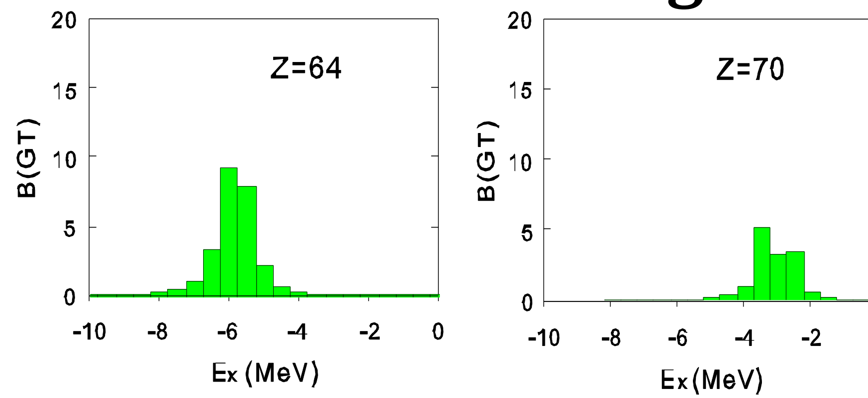

$\sum B(GT)=14.4$ $\sum B(GT)= 8.5$

Spin-dipole strengths: 1^-

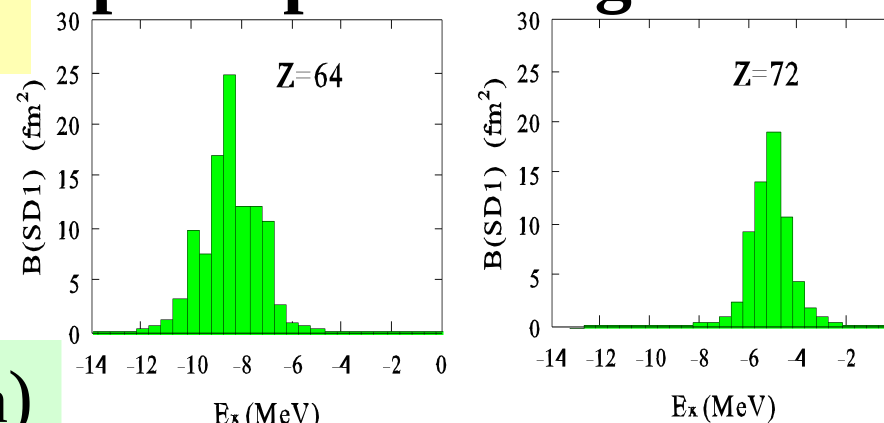

$\Sigma SD1=55.5\ fm^2$ $\Sigma SD1=40.1\ fm^2$

Beta-decay: GT + FF (first-forbidden)

Half-lives of N=126 isotones GT + FF (first-forbidden)

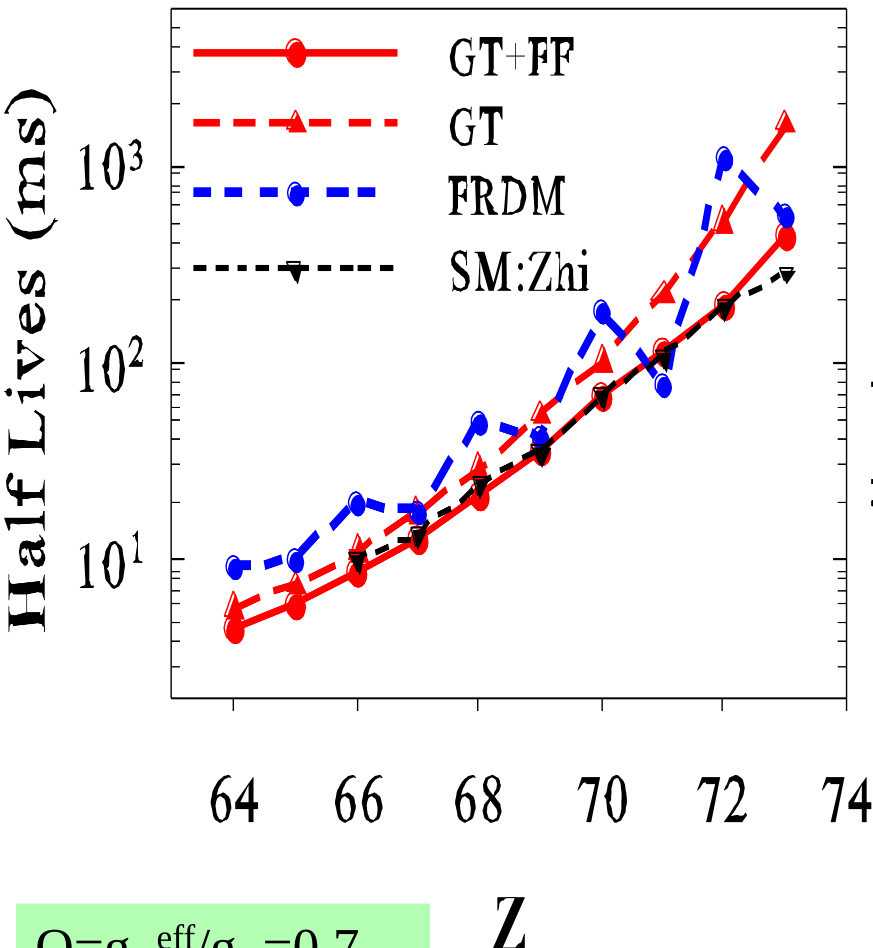

$Q=g_A^{eff}/g_A=0.7$

Suzuki, Yoshida, Kajino, Otsuka, PR C85, 014802 (2012)

r-process nucleosynthesis

Constant Entropy Wind Model

$T_9=(T_{09}-T_{\alpha 9})\exp(-t/\tau)+T_{\alpha 9}$

$T_{09}=9,\ T_{\alpha 9}=1\ ,\ \tau= 5.60$ ms

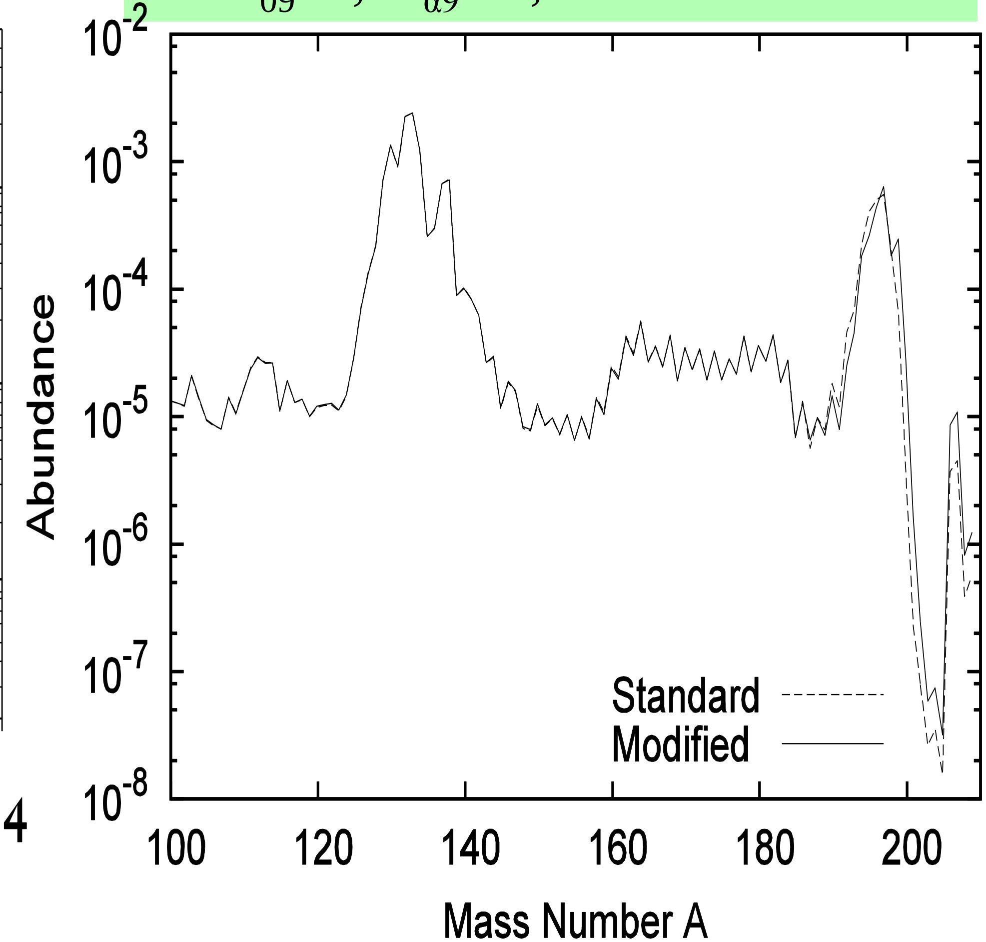

Half-lives:

Standard (Moller et al.)

Modified

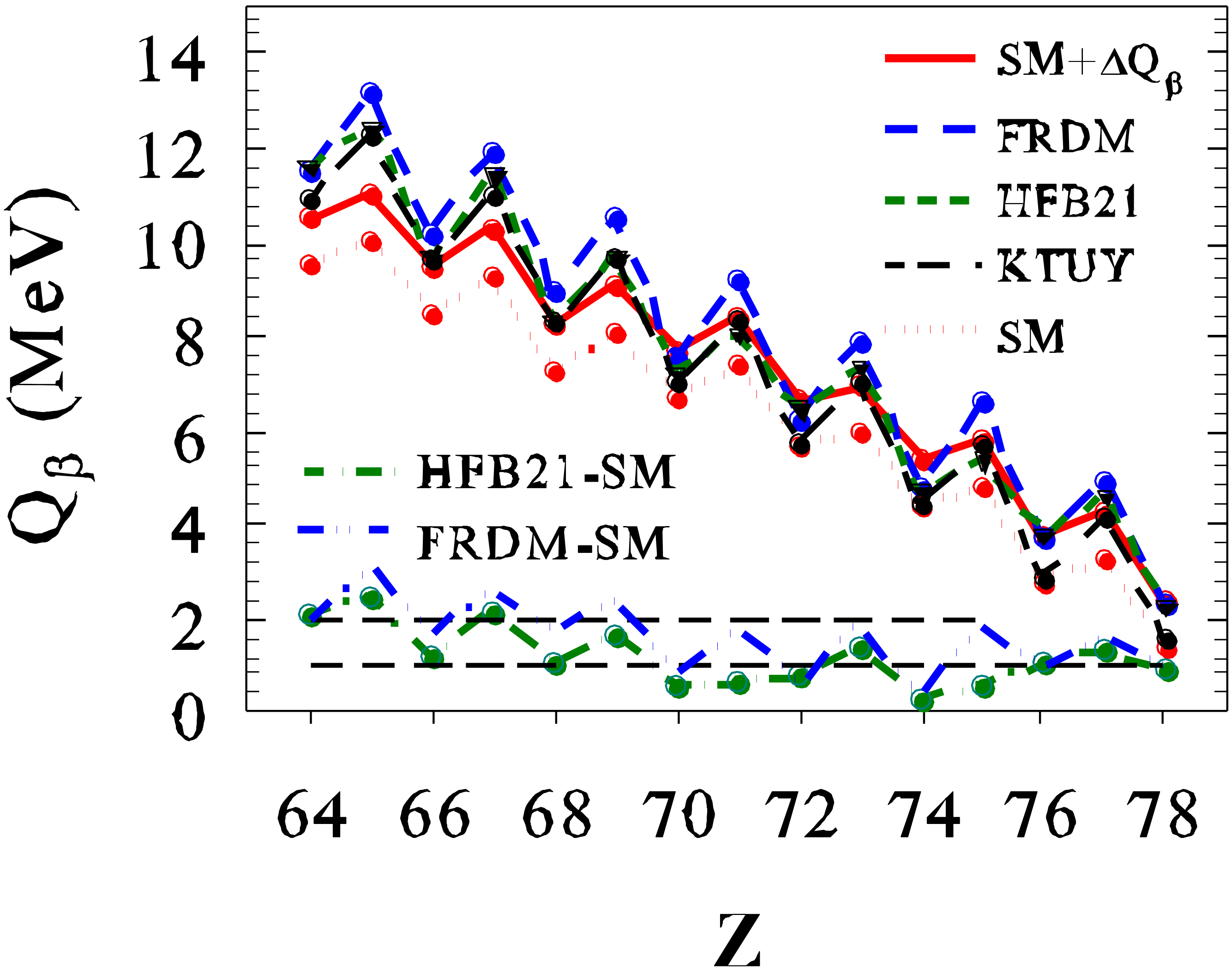
SM+ΔQ$_\beta$
FRDM
HFB21
KTUY
SM
HFB21-SM
FRDM-SM
Q_β (MeV)
Z
0
2
4
6
8
10
12
14
64
66
68
70
72
74
76
78

ΔQ = 1 MeV

r-process nucleosynthesis up to Th and U

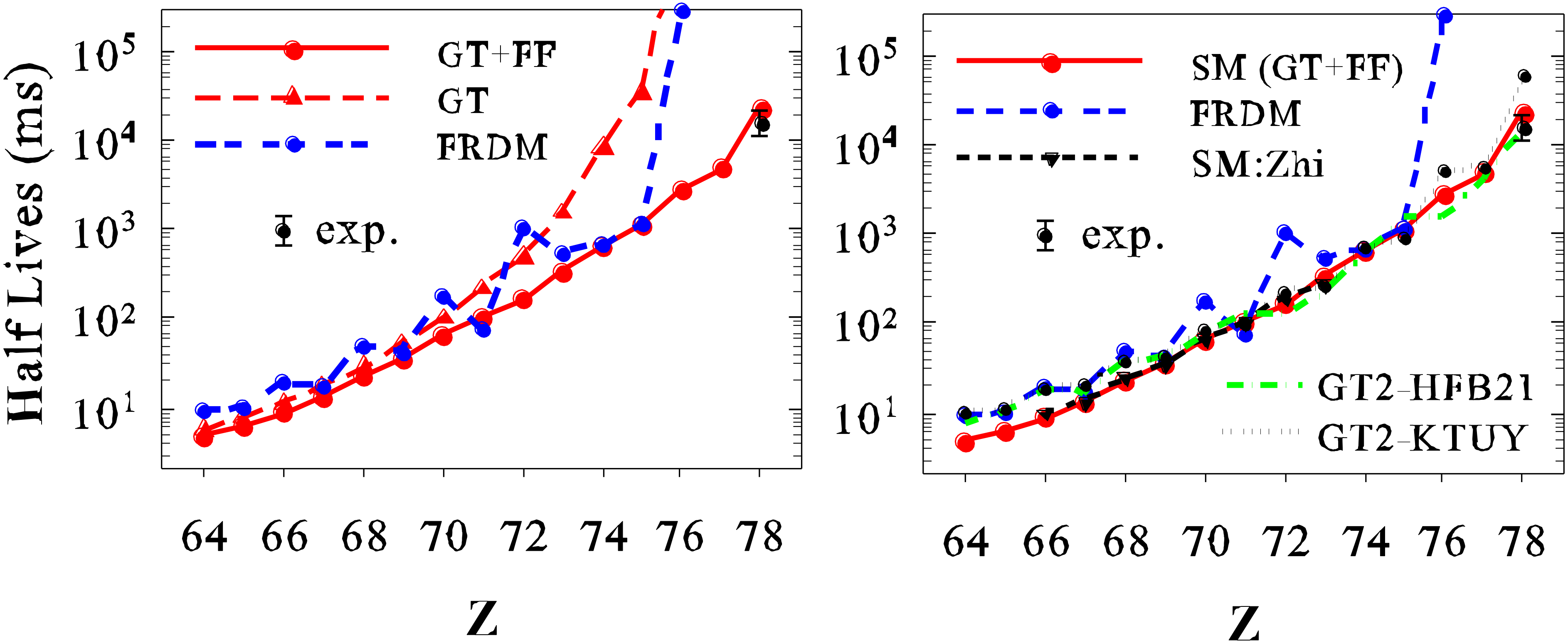

GT: $q(g_A)=0.7$

FF: $q(g_A)=0.34$, $q(g_V)=0.67$

Z=78: ^{204}Pt $t_{1/2}$(exp) =16 +6/-5 s Morales et al., PRL 113 (2014)

ν-driven-wind model in core-collapse SNe

Yoshida

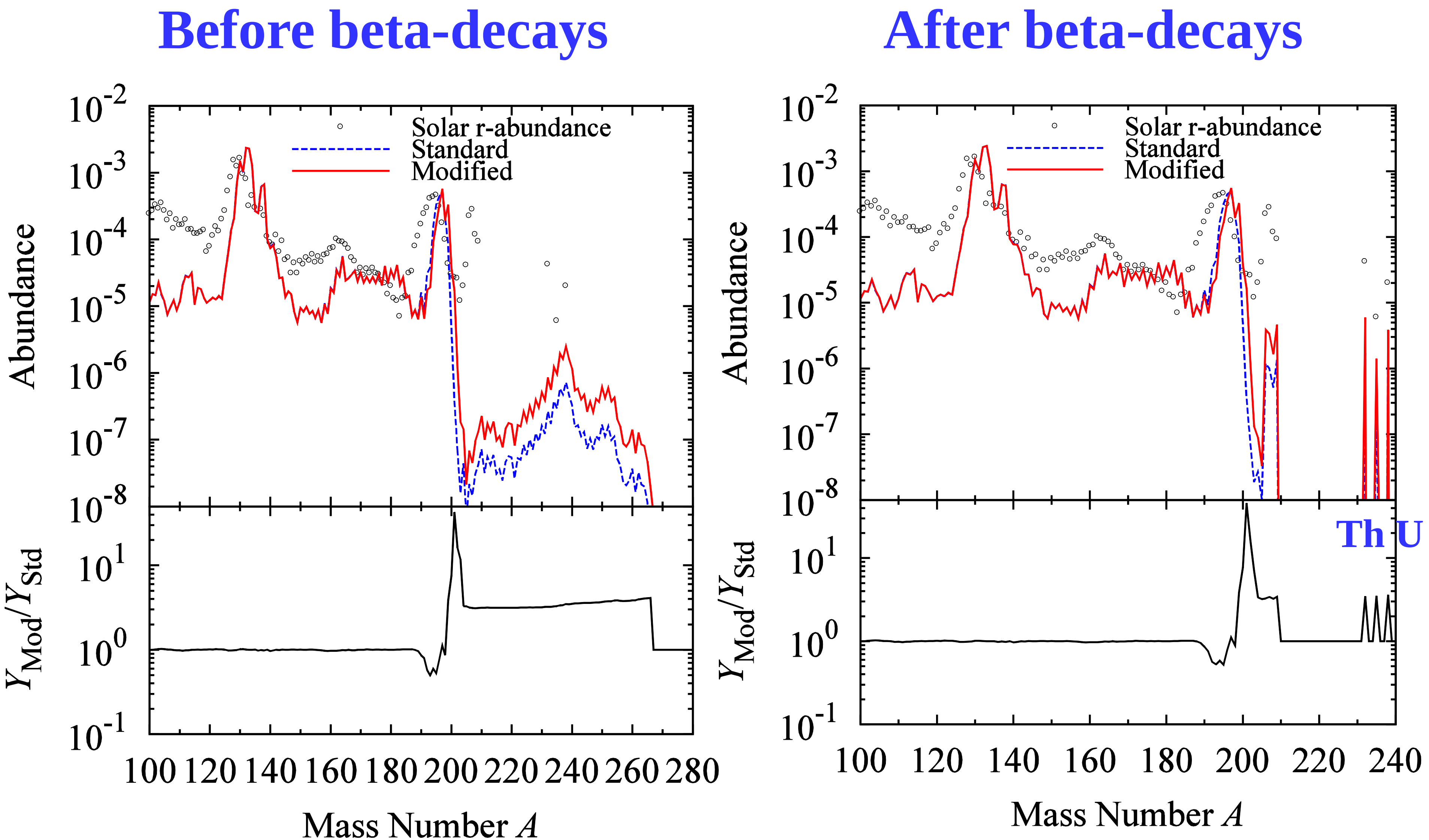

Standard = FRDM

Cold case: $T_f = 1\times10^8$ K

Before beta-decays

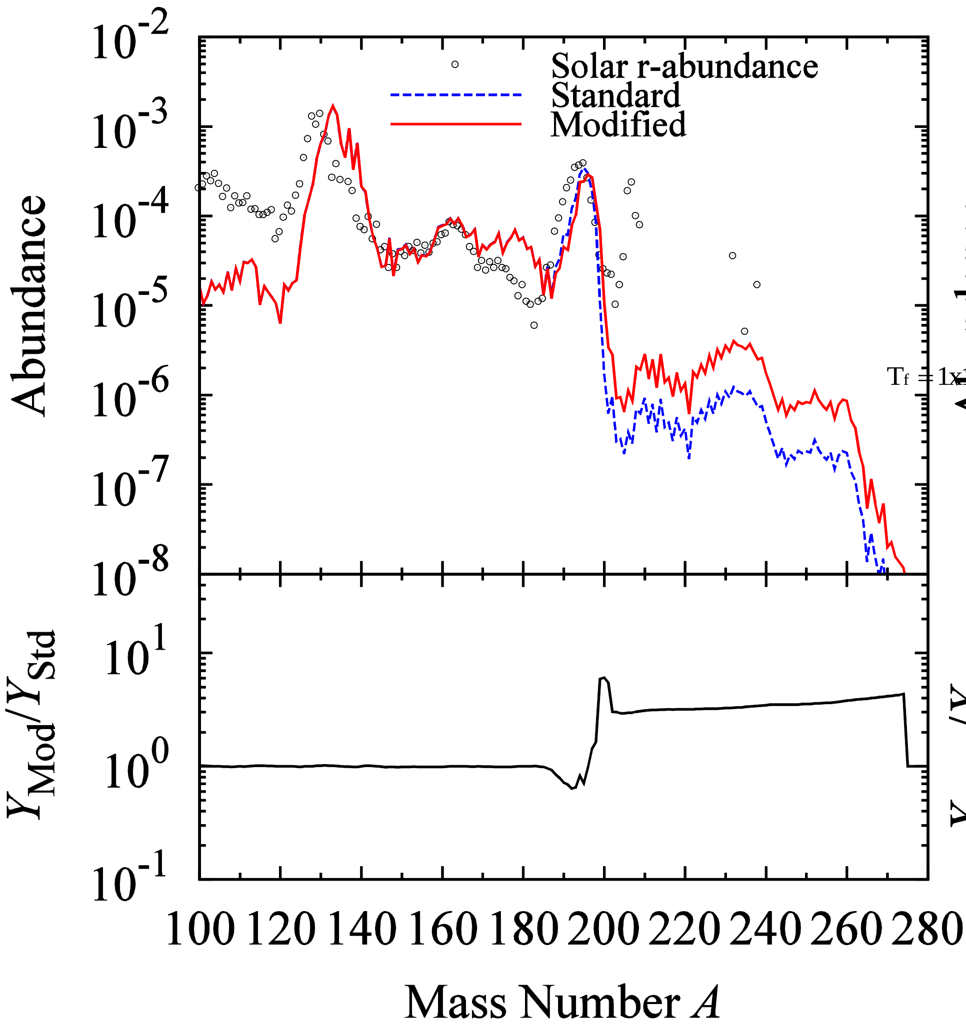

After beta-decays

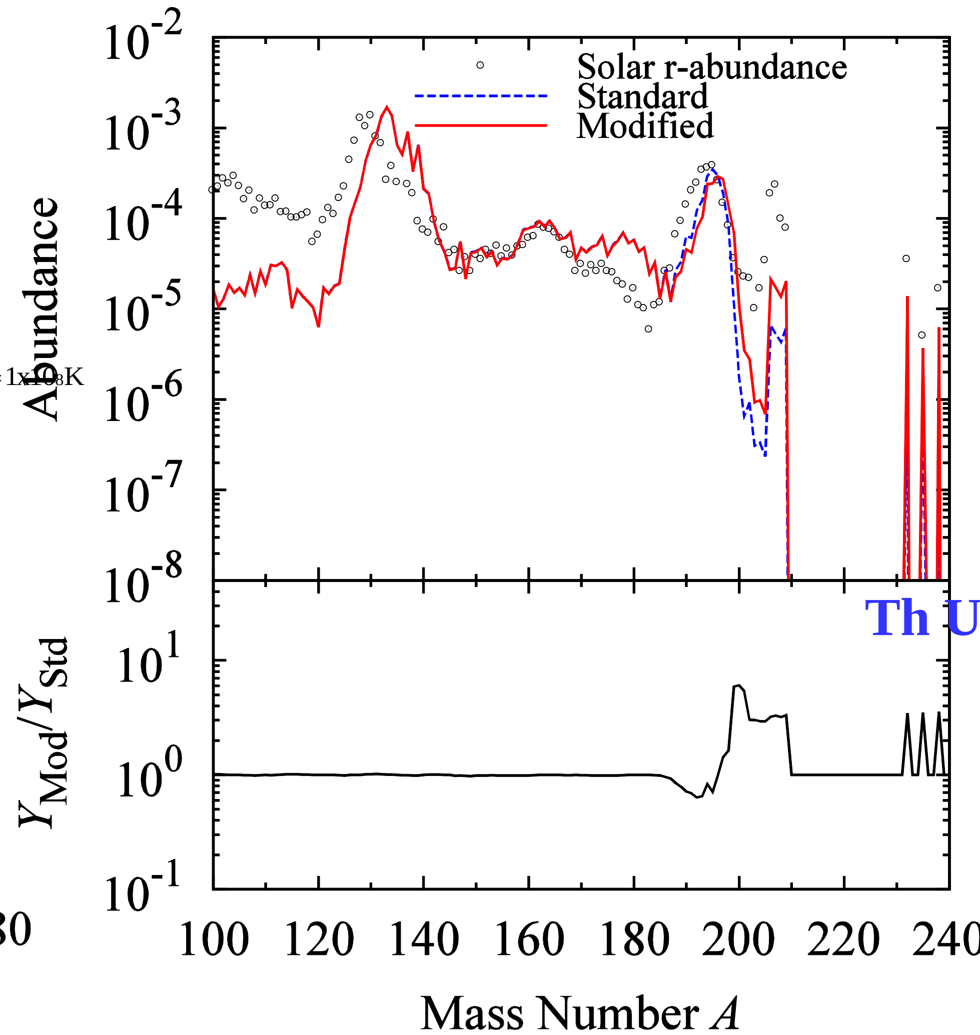

MHD-jet SNe

Shibagaki-Kajino

Before beta-decays

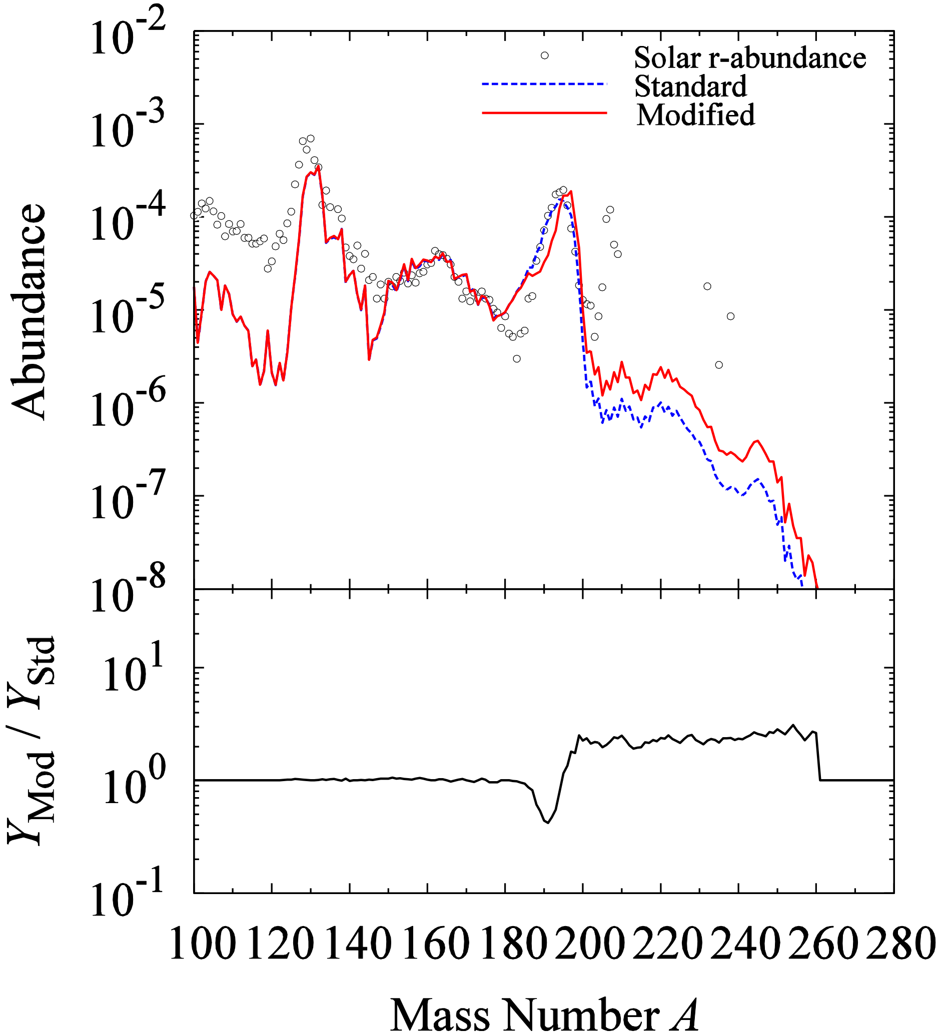

After beta-decays

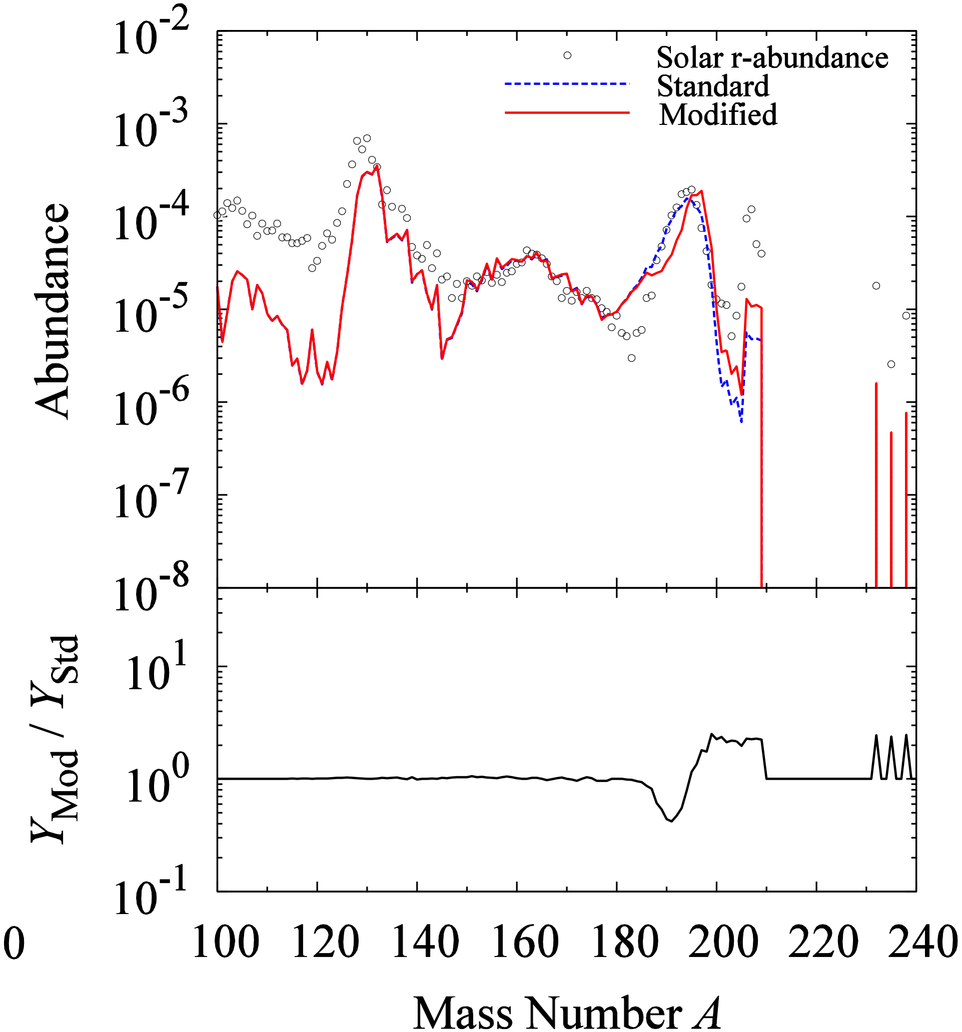

Standard = GT2-KTUY

r-process nucleosynthesis in neutron-star mergers

Shibagaki & Kajino

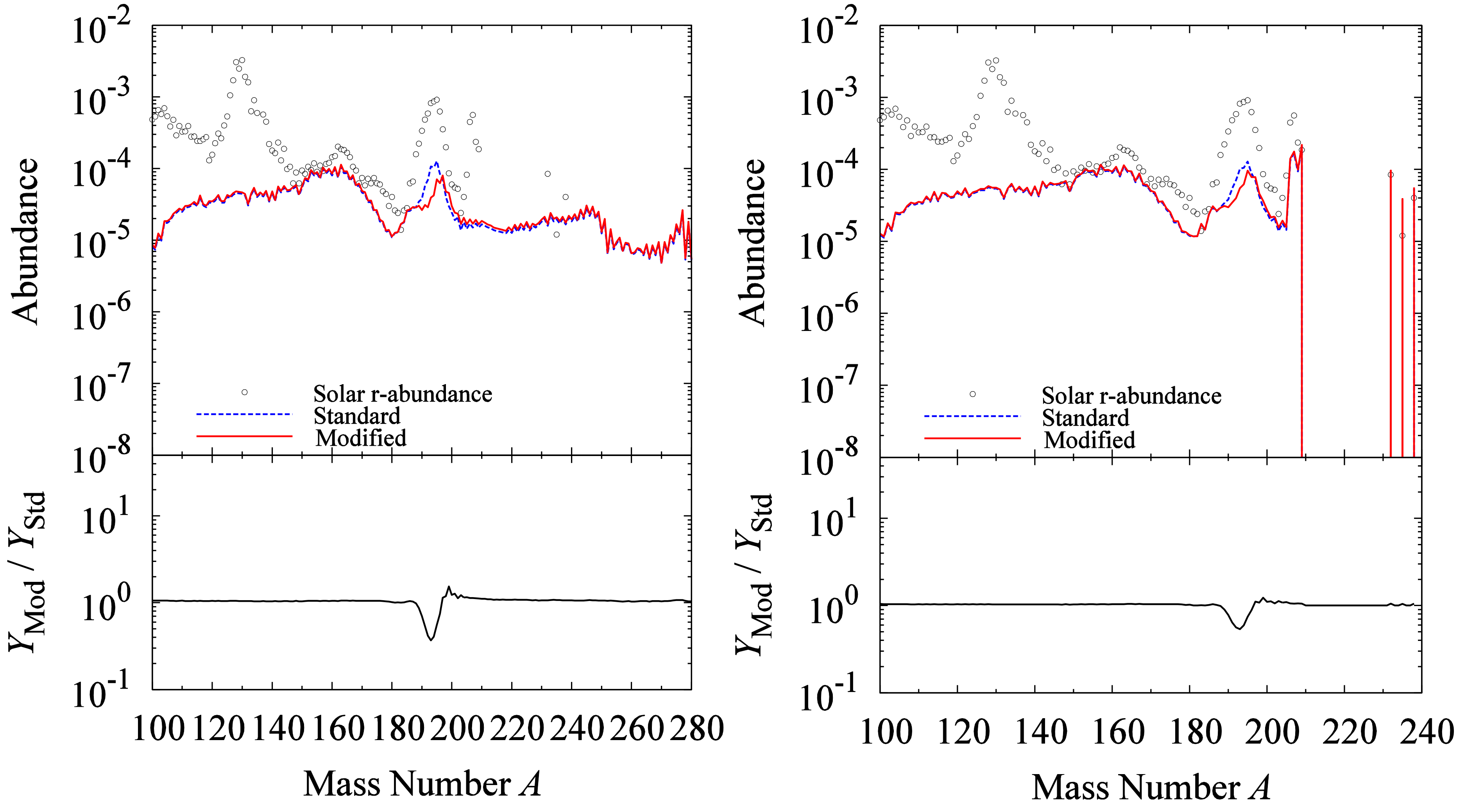

Standard = GT2-KTUY

r-process nucleosynthesis in neutron-star mergers

Wanajo

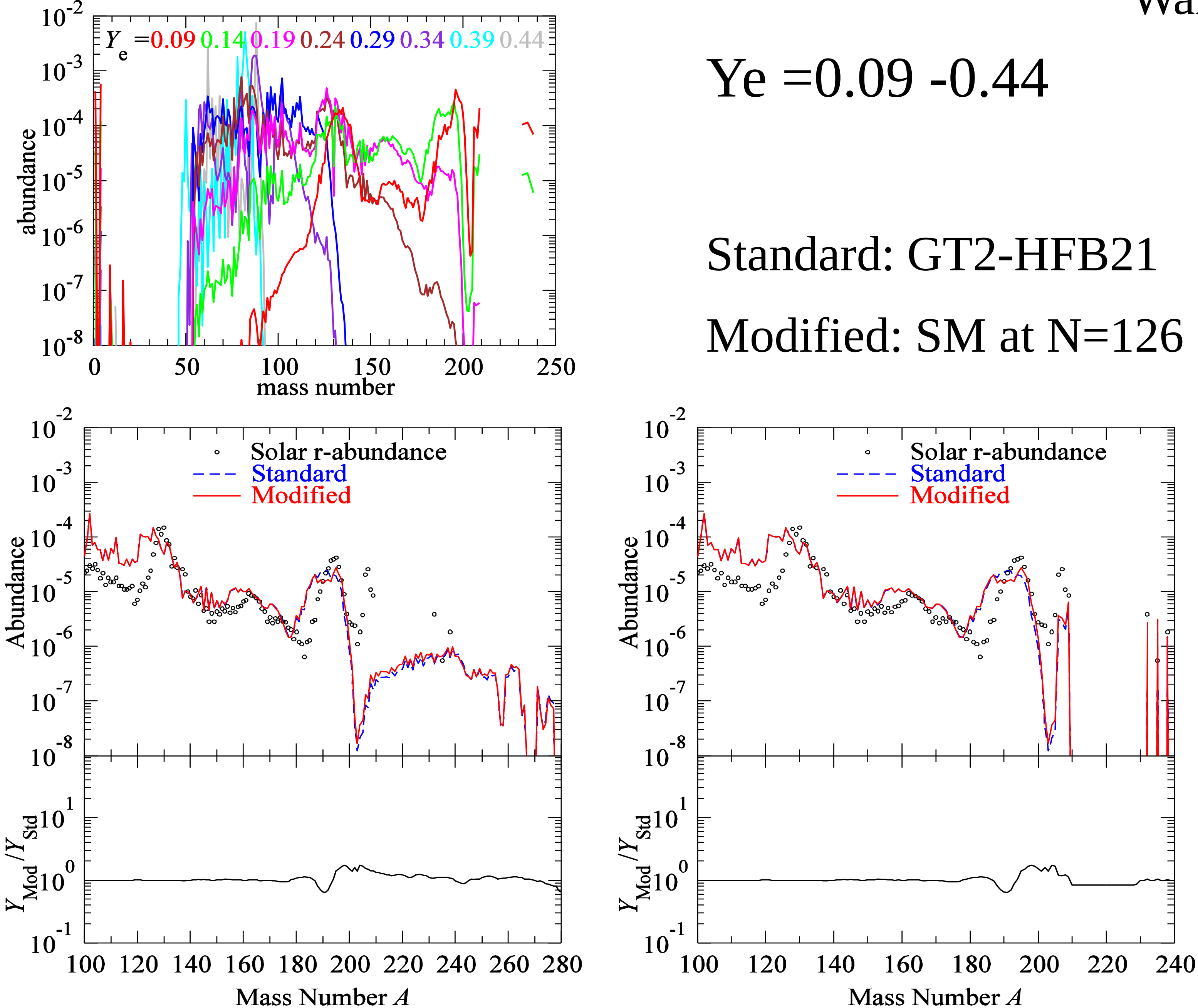

Ye =0.09 -0.44

Standard: GT2-HFB21

Modified: SM at N=126

Summary

- **New ν –induced cross sections based on new shell-model Hamiltonians (SFO for p-shell, GXPF1 for pf-shell)**

- **Good reproduction of experimental data for ^{12}C (ν, e^-) ^{12}N, ^{12}C (ν, ν') ^{12}C and ^{56}Fe (ν, e^-) ^{56}Co**

- **Effects of ν-oscillations in nucleosynthesis abundance ratio of $^{7}Li/^{11}B$ → ν mass hierarchy**

- **GXPF1J well describes the GT strengths in Ni isotopes : ^{56}Ni two-peak structure confirmed by recent exp.**

→ ▪ Accurate evaluation of e-capture rates at stellar environments
Nucleosynthesis in Type-I SNe; $^{58}Ni/^{56}Ni$ reduced

→ ▪ Enhancement of ^{56}Ni(ν, ν'p)^{55}Co reaction cross sections and production yield of ^{55}Mn in Pop III stars

- **Detailed e-capture and beta-decay rates for URCA nuclear pairs in 8-10 solar-mass stars**

→ URCA density for A=25 and 23 with fine mesh of density and temperature

→ Cooling of O-Ne-Mg core by nuclear URCA processes determines the fate of the stars.

- **URCA processes in neutron star crusts**
  ^{29}Mg-^{29}Na, ^{55}Ti-^{55}Sc pairs

- **Half-lives of N=126 isotones are evaluated by shell-model calculations with GT and FF contributions.**

→ Shorter half-lives than FRDM
r-process nucleosynthesis up to Th and U at SNe and neutron-star mergers

Collaborators

T. Kajino [a,b], M. Honma[c], T. Yoshida[d], M. Famiano
T. Otsuka[e], S. Shibagaki[a], S. Wanajo[f]
H. Toki[g], K. Nomoto[h], S. Jones[i], R. Hirsci[i]

[a]National Astronomical Observatory of Japan
[b]Dep. Of Astronomy, Univ. of Tokyo
[c]University of Aizu
[d]YITP, Kyoto University
[e]CNS and Dept. of Physisc, Univ. of Tokyo
[f]RIKEN
[g]RCNP, Osaka University
[h]WPI, the Univ. of Tokyo
[i]Keele University